THE IMPACT OF GLACIATION AND CLIMATE CHANGE ON BIOGEOCHEMICAL CYCLING AND LANDSCAPE DEVELOPMENT

James Brice Mabry

Submitted to the faculty of the University Graduate School
in partial fulfillment of the requirements
for the degree
Master of Science
in the Department of Earth Sciences,
Indiana University

December 2011

Accepted by the Faculty of Indiana University, in partial
fulfillment of the requirements for the degree of Master of Science.

_____

Gabriel Filippelli, PhD, Chair

_____

Kathy Licht, PhD

Master's Thesis
Committee

_____

Xianzhong Wang, PhD

ABSTRACT

James Brice Mabry

THE IMPACT OF GLACIATION AND CLIMATE CHANGE ON BIOGEOCHEMICAL CYCLING AND LANDSCAPE DEVELOPMENT

Lake cores from Dry Lake, California and Crystal Lake, Illinois were analyzed to identify climate variability and characterize landscape response to glacial/deglacial climate transitions.

Geochemical analysis of the Dry Lake sediment prior to the 8.2 kyr event revealed average values for percent total organic carbon to be 4% with a range of 0.2% to 15.2%. The average decreased to approximately 2.1% with a range of 0.4% to 5.3% during and after the event. Occluded phosphorus averaged 488 µg/g before the 8.2 kyr event and 547 µg/g after but was much lower during the event at 287 µg/g. These results were interpreted as an environment which began as warm, wet, and productive then quickly turned colder and drier during the 8.2 kyr event which resulted in a resetting of soil development. The higher temperatures returned after the 8.2 kyr event which allowed for continued soil development despite its drier climate. Previous research corroborated these conclusions.

The Crystal Lake geochemical record was very different from Dry Lake. Percent total organic carbon averaged 6.7% with a range of 3.9% to 8.5% during the Younger Dryas but recorded a lower average before and after at 4.9% and 4.6% respectively. Occluded phosphorus acted similarly with a higher average during

the cooling event, 2626 µg/g, and lower averages before and after, 1404 µg/g and 1461 µg/g, respectively. This was interpreted as continued productivity and soil development through the cold period which was attributed to a change in biomass.

Gabriel Filippelli, PhD, Chair

TABLE OF CONTENTS

LIST OF TABLES

LIST OF FIGURES

INTRODUCTION

Past climate studies have shown us that the earth's climate can change dramatically in a matter of decades (Alley et al., 2003). Even sporadic catastrophic weather events like floods and hurricanes can cost billions of dollars and even human lives, making it imperative that we understand natural climate changing processes. Unfortunately, reliable climate measurements (i.e., temperature and precipitation) cover only the last 150 years. The data collected in this relatively short period isn't extensive enough to draw adequate conclusions on changing climatic patterns. The geologic record of climate change stored in archives - ice and sediment - push back the climate record significantly.

Sediment cores taken from lakes allow us to identify climate anomalies which occurred thousands of years ago as well as to reconstruct local landscape responses to climate over thousands of years (Bradbury, 1986). The extensive data retrieved by the Antarctic and Greenland ice core projects have supplied high-latitude reference data on timescales of hundreds of thousands of years (Dowdeswell and White, 1995). Comparing the records from lake cores with that of the ice cores can give details on how extensive past climatic patterns were on a global scale, particularly at low latitudes. Two glacial lakes have been chosen as the setting of a multi proxy research project to uncover landscape response to glacial/deglacial transitions - Dry Lake in southern California and Crystal Lake in northern Illinois. The two sites have very different geomorphologies and rock and soil geochemistries. Furthermore, cores recovered from these lakes span different intervals of rapid climate change. These conditions allow the examination of

how nutrient cycles are affected by climate transitions of varying length and magnitude over very different landscapes.

Specifically addressed in this research are two abrupt cooling events: the 8.2 kyr event and the Younger Dryas (Fig. 1). The purpose of this research is to (1) create a high resolution data set which will identify climate variability during the late Pleistocene and early Holocene, (2) characterize the landscape response to glacial/deglacial climate transitions, and (3) examine the effect of the 8.2 kyr cooling event in western North America.

This research is part of a larger study covering North American climate change. Previous studies by Filippelli and Souch (1999) and Bird and Kirby (2006) have provided early Holocene climate data from Dry Lake. Crystal Lake has just recently been studied by Gonzales and Grimm (2009) whose work I will complement by focusing on the late Pleistocene Younger Dryas cooling event.

BACKGROUND

Glacial lakes that originated from melting glaciers are prominent in the northeastern and north central United States. These provide a valuable resource to assess local landscape development due to their limited drainage basin and minimal input from outside sources. Geochemical analysis of the sediment from a cored lake can provide a chronological cross section of changing landscape influenced by precipitation, temperature, biological activity, and even anthropogenic input.

Late Pleistocene/early Holocene climate events

The Crystal Lake core spans an interval including the Younger Dryas cooling event which lasted about 1300 years and is identified in the Greenland Ice Sheet Project Two (GISP2) as occurring between 12800-11500 calibrated years before present (cal yrs BP). The event is characterized as a period of decreased temperatures and precipitation in the North Atlantic region (Dowdeswell and White, 1995) but research shows the effects of the Younger Dryas were felt worldwide. Clapperton et al. (1997) used morphologic and stratigraphic evidence to prove the expansion of Andean ice caps in Ecuador which was ice free before and after the Younger Dryas. A Norwegian lake core revealed a sudden increase in bulk sediment input to the lake basin at the onset of the Younger Dryas and then an equally sudden return to pre-Younger Dryas conditions at 11700 cal yrs BP (Bakke, 2009).

Theories as to the cause of the Younger Dryas are disputed but it is thought to have originated from an interruption in the North Atlantic thermohaline circulation (THC) (Fairbanks, 1989). The THC is a product of density contrasts where water

warmed in the equatorial Atlantic travels northward along the surface. Fresh water is evaporated making the ocean saltier and denser. As it cools, this causes downwelling of the denser water mass forming North Atlantic deep water. An infusion of fresh water from a North American continental glacial lake could have reduced ocean salinity and interrupted the THC bringing Atlantic heat exchange to a stand still (Marotzke, 2000). A more recent theory credits a meteor which broke up in the earth's atmosphere, causing a reduction in solar radiation and temporarily returning the earth to glacial conditions (Firestone et al., 2007).

The focus of the Dry Lake research is the 8.2 kyr cooling event which was a 300 year episode of sustained colder temperatures during the post glacial recovery. It has been identified in previous research in the Dry Lake region (Bird and Kirby, 2006; Bird et al., 2009) and has been identified in this research as occurring between 8350-8070 cal yrs BP. The 8.2 kyr event was evident in the GISP2 ice cores as a decrease in average temperature (Alley, 1997), as enhanced precipitation in the South Pacific (Ljung, 2008), and as reduced seasonal monsoons in Asia (Rohling, 2005) and the mid east (Cheng et al., 2008). Evidence of the event has been observed in North America but to varying degrees (Bird and Kirby, 2006; Filippelli et al., 2006). Like the Younger Dryas, the cause of the 8.2 kyr event is disputed. The predominant idea among researchers is the catastrophic draining of glacial Lake Agassiz into the North Atlantic altering the thermohaline circulation (Hillaire-Marcel, 2007).

CLIMATE PROXIES

Phosphorus (P) is an important biolimiting nutrient which plays an essential role in soil productivity and thus plant growth (Filippelli, 2006). Its primary source is the mineral apatite therefore availability is dependent on the content in source rock and the degree of weathering (Schlesinger, 1997). Phosphorus can be utilized by plants but is also subject to interaction with other soil minerals. Some of these interactions can transform P into less available forms which significantly limits productivity. Previous work on sediment cores has shown that climate controls the rate of phosphorus weathering while the types of phosphorus present indicate biological metabolic influences (Vitousek et al., 1997; Filippelli et al., 1999).

The proportion of these P types can be connected to source rock, climate, and overall soil maturation (Filippelli, 2006). The different forms can be isolated by geochemical means, measured, and then used to interpret climate impact. I focused specifically on three forms:

1. the mineral form as weathered from apatite
2. the occluded form which is adsorbed into the oxide structures of Fe, Al, and Mn and is biologically unavailable to biota
3. the organic form which is taken up by plants

Figure 2, taken from Walker and Syers (1976), represents the change in soil P geochemistry over time. Newly exposed bedrock is comprised almost completely of the mineral form. Over time, occluded then organic forms dominate the soil as it develops. This also illustrates how total P decreases over time due to runoff. Without input sources, the P required for plant growth would depend on the recycling of organic P from

dead plants. This model of P evolution predicts the level of soil development during changing glacial periods whether in an alpine region (Dry Lake) or a midwestern plains region (Crystal Lake).

Percent total organic carbon (percent TOC) and percent total organic matter (percent TOM) can provide insights into productivity levels as well (Bird and Kirby, 2005; TOC and TOM are linearly related via a multiplication factor of TOM = TOC * 2.5). Increased levels of organics would indicate periods of temperate climate with ample precipitation and decreases would signify low productivity due to drier climate or a return to glacial conditions. Sharp spikes in organic matter may indicate elevated precipitation events where debris was washed into the basin.

Elemental Al and magnetic susceptibility can be indicators of terrigenous supply linked mainly to precipitation events (Bertrand et al., 2007). While studying lake core sediment from southern Chile, Bertrand et al. found a positive correlation between these three proxies and a drying period in Chile which corresponded to Dansgaard-Oeschger events recorded in the Greenland ice cores (Dowdeswell and White, 1995).

STUDY SITES

Dry Lake

Dry Lake (2763 m), Figure 3, is a moraine dammed alpine lake located in the San Bernardino Mountains in south central California (34.120460º N latitude, 116.827661º W longitude). Water volume and surface area vary significantly in response to precipitation variations. The majority of its water supply comes from winter precipitation in the form of spring melt. The watershed is limited at 3.7 km^2 but the relief varies by as much as 370 m. The surrounding peaks in the watershed and catchment basin are underlain by biotite gneiss, schist, and quartz monzonite and are covered with sparse coniferous forest (Bird and Kirby, 2006). Dry Lake lacks recorded meteorological data so it was taken from Big Bear Lake, about 18 km northeast, which has records from 1960 to present. Annual climate records show temperatures in the region average 8.2ºC with 55.6 cm of precipitation (Western Regional Climate Center, 2009).

Crystal Lake

Crystal Lake (273 m), Figure 4, is located in the town of Crystal Lake in McHenry County, Illinois approximately 45 miles northwest of Chicago (42.235831º N latitude, 88.344122º W longitude). It is a kettle lake with 0.9 km^2 surface area and a 12.4 km^2 watershed in a low relief setting. It formed during the Pleistocene deglaciation and is groundwater fed (Sasman, 1957). Its basement is dolomite bedrock covered by 60 m of sand and gravel overlain by laminated silt capped by a silt loam diamicton (Curry, 2005). Annual climate records show temperatures in the region average 8.9ºC with 92.7 cm of precipitation (Midwestern Regional Climate Center, 2000).

Charcoal, wood, and plant fragments were removed from samples from both sites and subjected to AMS (Accelerator Mass Spectrometry) radiocarbon dating and calibrated to calendar years before present as noted in the parent texts of Bird and Kirby (2006) for Dry Lake and Gonzales and Grimm (2009) for Crystal Lake. The remaining samples were dated assuming linear sedimentation rates between carbon dated samples. Figure 5 details the chronological data from Dry Lake, Figure 6 from Crystal Lake.

METHODS

Two cores totaling 8.4 m of sediment were recovered from Dry Lake, spanning 9000 cal yrs BP to present; collection methods are detailed in Bird and Kirby (2006). Grain size analysis was performed (Bird and Kirby, 2006) which revealed silt to be the main constituent throughout the core interbedded with sand in thicknesses of 1-10 cm, some capped with organic matter. Seven dates were eliminated due to rapid deposition events between 8900-6500 cal yrs BP.

Of the 700 samples, 87 samples were selected for analysis within the core depth of 307 cm-842 cm to ensure the 8.2 kyr cooling event would be analyzed (Fig. 5). The samples were spaced approximately 5-10 cm apart except for two 50 cm gaps at 7780-7739 cal yrs BP and 8141-8093 cal yrs BP where no samples were available. These gaps are attributed to the coring method but are accounted for in the age control process, as described at the end of this section, and assumed to be actual gaps in time and sedimentation (Bird and Kirby, 2006). Linear sedimentation is assumed between these gaps.

Two cores totaling 12.9 m of sediment were recovered from Crystal Lake spanning 16,000 cal yrs BP to 1000 cal yrs BP; collection methods are detailed in Gonzales and Grimm (2009). The Crystal Lake basement rock is Silurian dolomite bedrock under 60 m of clayey loam glacial diamicton, sand, and gravel overlain by 10 m of laminated silt and clay (Curry, 2005). Of the 932 samples, 80 samples were selected covering the depth of 1750 cm-2222 cm to ensure the Younger Dryas cooling event would be analyzed (Fig. 6).

After selection, the samples from both sites were processed in the same manner. They were initially dried using the Virtis Benchtop freeze drier. Approximately 0.5 g of each dried sample was transferred into crucibles and ashed at 550ºC in the FisherScientific Isotemp Muffle Furnace. The samples were reweighed and the percent total organic carbon (percent TOC) was calculated.

Approximately 0.1 g of each ashed sample was put into 100 mL microwave vessels with a mixture of HNO_3, HF, and HCl acids and digested fully in the CEM MDS 2000 microwave. The digested samples were diluted and analyzed for elemental content using the Leeman Labs Inductively Coupled Plasma Spectrometer PS950. Each sample was scanned three times for Al, Ba, Ca, Fe, K, Mg, Mn, Na, P, Sr, Ti, and Zn. The scans were recorded in parts per million (ppm), averaged, and the percent error determined (Tables 1 and 2). A subset of digested Crystal Lake samples were also analyzed for Ir in the manner described above but the detection level of the equipment was insufficient to record meaningful levels of Ir.

Approximately 0.1 g of dried sample was subjected to a four step extraction technique, modified from Tiessen and Moir (1993), to separate the phosphorus component into geochemically similar pools. (1) A sodium dithionite reducing agent was used to release occluded phosphorus from its iron oxide lattices. The solution was decanted, rinsed with $MgCl_2$, decanted again, and the supernatant saved. (2) The biogenic mineral fraction was dissolved with a buffered sodium acetate solution. After decanting, the sediment was rinsed twice with $MgCl_2$, decanted, and the supernatant saved. (3) The remaining mineral fraction was dissolved using 1 M HCL. The solution was decanted and the supernatant saved. (4) A combination of a $MgNO_3$ solution and

ashing at 550ºC was used to remove the organic matter and free the phosphorus associated with it. The remaining sample was rinsed in 1 M HCl, centrifuged, decanted, and the supernatant saved.

The occluded fraction was measured in the Leeman Labs Inductively Coupled Plasma Spectrometer in the same manner as the digested samples described above. The biogenic, mineral, and organic fractions required further manipulation and were measured using a colorimetric technique. This was based on the reaction of phosphate with ammonium molybdate and antimony potassium tartrate under acidic conditions. When the solution was subjected to ascorbic acid, the phosphate content became discernable by forming a blue complex which absorbs light at 880 nm. The magnitude of color was measured with the Shimadzu UV-2401PC spectrophotometer. All fractions were measure in triplicate, mean and standard deviation calculated with percent error recorded as standard deviation from the mean (Tables 1 and 2). Average percent error for all P fractions is 3%.

After analysis, the results for the biogenic (2) and mineral (3) fractions were added together and recorded as one complete mineral fraction. The phosphorus extraction data was recorded in µg/g then converted into percent of total phosphorus. This method is suitable as the drainage basins of Dry Lake and Crystal Lake are relatively small, especially in the case of Dry Lake, and therefore considered closed systems ecologically.

RESULTS

Dry Lake

In terms of concentration, the occluded phosphorus fraction is the dominant form averaging 469 µg/g and appears to be the most variable (Fig. 7). The mineral and organic forms, averaging 181 µg/g and 82 µg/g, respectively, have significantly lower variability and vary directly at the top and bottom of the core but are inversely related during the period 8200-7200 cal yrs BP.

The oldest part of the core displays a great degree of variability in the occluded fraction from about 8900 to 8350 cal yrs BP (Fig. 7), whereas the mineral and organic fractions are relatively constant. Following this is an interval of low and relatively constant occluded P fraction from 8350 to 7700 cal yrs BP. At approximately 7700 cal yrs BP occluded P reverts to the variability as seen in the older part of the core. The concentrations of mineral and organic P vary little during this period appearing relatively flat compared to the earlier record.

The percent TOC curve (Fig. 7) characteristics mimic those associated with the occluded phosphorus concentration data in that there is a greater degree in variation at the bottom of the core averaging 4% with two major spikes at about 8850 cal yrs BP and 8500 cal yrs BP. There is also the similar flattening of the curve between 8100-7800 cal yrs BP. From this point to the youngest part of the core, percent TOC values are relatively lower and demonstrate less variability with fewer peaks.

In terms of percent total P (Fig. 8), the occluded fraction is dominant averaging 61%. The organic and mineral fractions average 11.3% and 26.7% respectively. There is an observed decrease in occluded P to 56% from approximately 8300-7700 cal yrs BP.

Prior to 8300 cal yrs BP and after 7700 cal yrs BP occluded P averages 61.5% and 69% respectively. Like the occluded P concentration in Figure 7, levels at the top and bottom of the core show a higher degree of variability while the period from 8300-7700 cal yrs BP appears more stable. Occluded P is only surpassed by the mineral fraction at one point, 8451 cal yrs BP. The period from 7422 cal yrs BP to the top of the core displays relative stability with only one substantial peak at 7091 cal yrs BP. The percentages of mineral and organic P tend to decrease and become more stable after 7700 cal yrs BP.

The ratio of occluded phosphorus concentration to mineral phosphorus concentration curve (Fig. 9) is analogous to the occluded P curve in Figure 8 averaging 2.6 with a range of 7.8 and an amplified peak of 8.7 at 7623 cal yrs BP.

The Al concentration (Fig. 10) varies consistently throughout the length of the core averaging 96300 μg/g with substantial peaks at 8893, 7579, and 7004 cal yrs BP.

Crystal Lake

The Crystal Lake record spans the Younger Dryas, and reveals several significant features. Occluded P is the dominant fraction averaging 1676 μg/g, followed by mineral P averaging 320 μg/g, with organic P representing the smallest fraction averaging 49.6 μg/g (Fig. 11). The earliest 1400 years of the core show a relative stability in all P fractions whereas values, particularly of occluded P, are higher and variable from about 14200 to 11000 cal yrs BP (Fig. 11). Values become more stable at the top of the record although the occluded P fraction remains at a higher level than at the bottom of the core. Organic P is easier to see in Figure 12 where initially it is relatively high, averaging 69 μg/g, but exhibits a decreasing trend through the end of the core.

Organic P is the lowest proportional fraction averaging 3% through the measured length of core, where occluded P is the greatest portion averaging almost 80% (Fig. 13). An overall trend of increasing proportion of occluded P and decreasing mineral P is seen throughout the sampling time period. There is great variability in all fractions at 14100 cal yrs BP, with organic P reaching its peak of 11%, and at 12700 cal yrs BP where mineral P comprises 50% of the total. A smaller peak occurs at 11700 cal yrs BP after which the fractions appear to stabilize. There is some variability for the last 2000 years of the record but the changes are gradual with the mineral fraction at its lowest level and occluded P at its highest.

Percent TOC (Fig. 11) averages 5.2% with the highest measurement of 9.8% at 14158 cal yrs BP and the lowest of 1.5% at 14105 cal yrs BP. The shape of the curve is similar in characteristics to the occluded P fraction curve, as was seen in the Dry Lake samples (Fig. 7), with less variability at the top and bottom of the core and a period of increased values and variability from 14200 to 11000 cal yrs BP. This period of variability is also illustrated in the GISP2 $\delta^{18}O$ data (Fig. 11) but appears to lead TOC and the P data by approximately 500 years.

The ratio of occluded phosphorus concentration to mineral phosphorus concentration (Fig. 14) is similar to the occluded P curve in Figure 13, averaging 7.0 with a range of 18.

The Al concentration (Fig. 15) varies more in the first half of the core sample averaging 10678 μg/g. The segment of the core prior to 14200 cal yrs BP displays the highest concentrations with peaks at 14890 and 14434 cal yrs BP with a record low level at 13785 cal yrs BP.

DISCUSSION

Dry Lake

The motive for using Dry Lake was to find a time capsule-like environment which would record local climate and landscape phenomena with minimal input from outside sources. Its limited drainage basin provided this setting and the elevation is a benefit to record glacial events and limits airborne particulate percent TOC.

Prior to the 8.2 kyr event

The percent TOC record prior to the 8.2 kyr event (Fig. 7) shows the highest range of values including the core record minimum of 0.23% at 8651 cal yrs BP and two spikes, one reaching 15% at 8870 cal yrs BP and another above 14% at 8501 cal yrs BP. This corresponds to the variability of the P record (Fig. 7) over the same period with peaks in occluded P and minimum values of organic P. This interprets as a warm and climatically volatile period, more so than the later core record, with various erosion events as seen in percent TOC and the increased elemental Al record (Fig. 10). This agrees with the assessment of Bird and Kirby (2006) of an enhanced North American Monsoon (Fig. 16) with (1) increases in percent TOM - evidence of increased temperatures encouraging biomass, (2) spikes in percent sand - confirming precipitation events, and (3) suppressed CHI - a result of basin productivity resulting in oxidation of the magnetic fraction by bacterial processes.

Taking a closer look at the spike at 8501 cal yrs BP, the increase in percent TOC and occluded P begins at approximately 8574 cal yrs BP and increases continuously to 8501 cal yrs BP where both begin a decline to 8451 cal yrs BP. In terms of proportion of

total P (Fig. 8), this 70 year interval is marked by an increasing percentage of occluded P and decreased mineral P. The following 50 year interval exhibits the opposite trend, ending with the one point in this data where the percent mineral P exceeds percent occluded P as well as where percent organic P reaches its highest level. Collectively, this 120 year period could be explained as sustained, though short-lived, soil development attributed to warmer temperatures, increased precipitation, and basin productivity. An interpretation of increased precipitation is consistent with increased percent sand (Fig. 16) and with low CHI values, which could also be a product of a warmer, more productive interval.

8.2 kyr event

The beginning of the 8.2 kyr event is marked by continued variability but lower values for percent TOC and occluded P concentration (Fig. 7). The small peaks in percent TOC correspond with peaks in occluded P at 8189 and 8069 cal yrs BP as well as increases in percent sand recorded by Bird and Kirby (Fig. 16) signaling possible precipitation events, although to a lesser degree than was seen previously. In terms of percent total P (Fig. 8), the variability continues through the 8.2 kyr event and all three fractions maintain very similar percentages from the bottom of the core through the event.

Prior to the 8.2 kyr event, the sediment accumulation rate averaged 0.36 cm/yr (Fig. 17) whereas within the event the average increases to 1.17 cm/yr. This could be attributed to an increase in precipitation which would increase detritus into the Dry Lake basin, as suggested by the increase in percent sand and CHI spikes (Bird and Kirby,

2006). If precipitation increased, an increase in mineral P concentration and possibly percent TOC (Fig. 7) would be expected but is not seen. One possible explanation for an increase in erosion is a return to glacial conditions, with concomitant decreases in protective plant cover.

Bird and Kirby (2006) made the same conclusion reasoning that the return to glacial conditions and decreased monsoonal precipitation caused a decrease in biomass therefore increasing erosion. Their findings in Figure 16 support these conclusions by elevated magnetic susceptibility (CHI) and percent sand, and a decrease in percent TOM. What is unexplained is why there was no increase in the mineral form of the phosphorus fraction to accompany the influx of sand and magnetic detritus (Fig. 7).

After the 8.2 kyr event

At the conclusion of the 8.2 kyr event, percent TOC and all the P fractions appear to remain consistently low for a 260 year duration (8060-7800 cal yrs BP) but that period is represented by only three data points, of which the end two points (8060 and 7800 cal yrs BP) are carbon dated (Fig. 5). Though samples are collected in approximately 5-10 cm intervals, the rate that sediment accumulated within each centimeter varies and thus the number of years of accumulation within each centimeter varies. The average rate of sediment accumulation over the entire data set is 0.48 cm/yr but within those two carbon dates the average is 0.05 cm/yr (labeled as point 'a' in Figure 17). There is no indication of an anomalous climate event from the GISP2 ice core or Bird and Kirby (2006) to account for this. This period is preceded and followed by 50 cm gaps in the sediment record (Fig. 5) as well as periods with sedimentation rates much higher than the core

average (labeled as points ‘b’ and ‘c’ in Figure 17 and measuring 1.02 cm/yr and 1.17 cm/yr respectively). A plausible conclusion is that one of the carbon dates is wrong. If either of the two carbon dates is disregarded, the sedimentation rate decreases to approximately 0.3 cm/yr which is closer to the core average of 0.48 cm/yr.

After 7700 cal yrs BP the percent TOC, mineral P, and organic P become relatively stable, a trend sustained through the end of this data set to approximately 6900 cal yrs BP (Fig. 7). Occluded P displays an increasing trend, both in concentration (Fig. 7) and as a percentage of total P (Fig. 8). Mineral and organic P percentages (Fig. 8) exhibit decreasing trends with the mineral fraction averaging 19% during this period versus 30% for the earlier portion of the core. Higher occluded P is an indication of progressive soil development with increased values often signaling increases in precipitation but when associated with lower mineral and organic P and lower percent TOC, it points to a drier period of warmer, stable temperatures allowing more advanced soil development than seen previously. This is perhaps a restrained equilibrium as is seen in Figure 2. This corresponds to Bird and Kirby (2006) which recorded depressed percent TOM and CHI (Fig. 16) along with a decreased and more stable percent sand record.

The ratio of occluded phosphorus concentration to mineral phosphorus concentration was included (Fig. 9) as a comparison to the occluded P curve in Figure 8. Figure 8 is a ‘closed system’ diagram, meaning that in order for one component to increase, another must decrease. Using the ratio in Figure 9 removes this closed system limitation and allows one more comparison of the data curves. The curve in Figure 9

exhibits noticeable differences in magnitude but mimics the Figure 8 occluded P curve in terms of contour with no substantive differences between the two.

Crystal Lake

The Crystal Lake setting is vastly different from Dry Lake in terms of altitude, source rock, terrain, and time frame measured but similar in that the Crystal Lake core data also encounters a climate anomaly as is seen in the data in Figure 11 and by Gonzales and Grimm (2009) in Figure 18.

Oldest Dryas (bottom of core-14700 cal yrs BP)

The earliest portion of the core from approximately 15600-14200 cal yrs BP covers the end of the Oldest Dryas stadial (Fig. 18). The percent TOC curve (Fig. 11) is flat and consistently low signaling an environment not conducive to biomass growth. There is little variation in P concentration (Fig. 11) with all fractions remaining low and consistent for the 1400 year period. The organic fraction is relatively low averaging less than 7% of total P (Fig. 13) but is at its highest percentage and concentration (Fig. 11) for the core record. These indicators point to a period of low temperatures without significant precipitation events, hindering biomass and the development of soil. Using *Picea* pollen data, Gonzales and Grimm (2009) concluded that the period was wetter than average as the *Picea* variant, a type of spruce, favors cold, wet conditions which they attributed to the proximity of the Laurentide ice sheet. In agreement with the conclusions of Gonzales and Grimm is the elemental Al record (Fig. 15) which records its highest

levels during this period, an indicator of increased accumulation into the lake, most likely from glacial debris.

The $\delta^{18}O$ record from GISP2 (Fig. 1) and the NGRIP (Northern Greenland Ice Core Project) from Figure 18 both record more negative $\delta^{18}O$ values, which would be consistent with lower temperatures during this period, but they also display a high degree of variability which is not reflected in the Crystal Lake P or percent TOC record. This may be due to the mid-continent location of Crystal Lake being somewhat buffered from ocean-driven variability.

Bølling/Allerød (14700-12800 cal yrs BP)

At approximately 14200 cal yrs BP percent TOC and all P fractions increase (Fig. 11) and begin a 2000 year period of increases in content and variability corresponding to the Bølling/Allerød interglacial. This period is identified in the GISP2 and NGRIP $\delta^{18}O$ data as beginning approximately 14600 cal yrs BP therefore the conclusion is that the Crystal Lake data displays a 300-400 year lag which Gonzales and Grimm (2009) attributed to the proximity of the Laurentide ice sheet causing lake effect temperatures and affecting productivity in the local area. The data presented here for percent TOC, P, and Al supports their findings with an identified lag.

The 60% spike in percent TOC at 14158 cal yrs BP indicates a rapid increase in temperature to encourage and sustain biomass. This is corroborated in the GISP2 ice core record by an increase from -41 at 14700 cal yrs BP to -36.5 at 14500 cal yrs BP, lag time considered. This 14150 cal yrs BP boundary at Crystal Lake is represented in Gonzales and Grimm (2009) by increases in organic carbon (Fig. 18) and *Fraxinus nigra*

(black ash) pollen which requires a warmer, wet climate. Also seen are increases in the deciduous *Ulmus* and *Quercus* pollen types, which require warmer temperatures, and a decrease in the spruce variant *Picea* which requires colder temperatures.

As percents of total P (Fig. 13), this period begins a decline in mineral and organic P with occluded P making up the bulk of the P content and increasing through the end of the core record. The spikes in organic and mineral P concentration (Fig. 12) at 14158, 13493, 13389, and 12703 cal yrs BP could be interpreted as input from the shrinking Laurentide ice sheet. If terrigenous material from the Lake Michigan Lobe of the Laurentide was draining into the lake basin, it should be indicated by corresponding peaks in elemental Al but the peaks are not present (Fig. 15). In fact, elemental Al decreases from its elevated levels prior to 14200 cal yrs BP. This could be explained by the receding ice sheet and overall increase in development of the soil with Al input coming increasingly from local sources.

Younger Dryas (12800-11500 cal yrs BP)

This period is marked by a change in the percent TOC and occluded P curves (Fig. 11) continuing from approximately 12700-11100 cal yrs BP further confirming the climate lag behind the Greenland ice core data identified by Gonzales and Grimm (2009). The occluded P records much higher levels and more enduring cycles than the period prior to. These peaks do not correspond with peaks in organic and mineral P concentrations or percent TOC.

Organic P decreases (Fig. 12) during the Younger Dryas from an average of 3.46 µg/g during the Bolling/Allerod to 1.83 µg/g, consistent with inhibited lake shed

productivity due to a decrease in temperatures. In contrast, percent TOC (Fig. 11) increases during the Younger Dryas from an average of 5.19 µg/g during the Bolling/Allerod to 6.30 µg/g. This is indicative of deeper soil formation rather than lake production as concluded by Filippelli et al. (2006). As a percentage of total P (Fig. 13), occluded P continues to increase and mineral P to decrease signifying soil more responsive to further development (Fig. 2) and less influenced by changing climate.

Gonzales and Grimm (2009) observed a decline in the abundance of the deciduous *Fraxinus* pollen (Fig. 18), which thrived during the Bolling/Allerod, and a recovery of the spruce *Picea.* Although the Younger Dryas stadial is established as a "return to glacial conditions" the Midwest was experiencing continued soil development and substantial plant productivity. The colder climate did not shut down landscape development, only facilitated the change in flora from deciduous forests to evergreen.

There was an attempt to locate iridium in a subset of samples to corroborate the findings of Firestone et al. (2007). Established crustal background values for Ir are less than 0.3 ppb if discernible at all (Alvarez et al., 1980). Values along the Cretaceous-Tertiary boundary have recorded from 20-160 times the normal background levels in 3 sample areas worldwide (Alvarez et al., 1980) and higher-than-background levels (<1-51 ppb) in six North American locations (Firestone et al., 2007). Crystal Lake tests were inconclusive revealing background levels well above what is considered normal which is attributed to limits of the testing equipment.

After the Younger Dryas (11500-9000 cal yrs BP)

Notable on Figure 11 is the sustained decrease in percent TOC and occluded P at approximately 11000 cal yrs BP. The decreasing trend in percent TOC and all fractions of P concentrations appears to correspond with the increase in GISP2 $\delta^{18}O$ data signifying an abrupt and sustained warming phase beginning approximately 11600 cal yrs BP. In Gonzales and Grimm (2009) this period is marked by the disappearance of the spruce pollen, *Picea*, (Fig. 18) and the increase in pollen types associated with deciduous forest.

As percents of total P (Fig. 13), all 3 fractions appear to stabilize reaching apparent equilibrium further along the soil development curve from Figure 2. The sustained decrease in mineral P (Fig. 12) and Al input (Fig. 15) represents a change in sediment source material from glacially derived to local soil erosion.

There are substantial gaps in sampling in this section of the record which may be responsible for the apparent smoothing of the curve but it is corroborated by the higher-resolution percent TOC curve from Gonzales and Grimm (Fig. 19). The organic P fraction is consistently lower than the mineral fraction in both the Crystal Lake and Dry Lake samples, not following the Walker and Sayers model for soil P over time (Fig. 2). There are two possible causes for these low values. First, the soils may be rich in iron, manganese, or aluminum oxyhydroxides which could encourage more of the available P to form the occluded fraction. The second issue may be the aggressive four step extraction technique which releases the fractions in sequential steps. As occluded is the first fraction to be released and decanted, it is possible some of the other fractions are dissolved and combined with the occluded fraction.

Like the Dry Lake section, the ratio of occluded phosphorus concentration to mineral phosphorus concentration was included (Fig. 14) as a comparison to the occluded P curve in Figure 13 and to remove the issues with a closed system diagram. The ratio curve is symmetrical to the occluded P curve in Figure 13 with relative differences in amplitude but no substantive differences between the two.

CONCLUSIONS

The high resolution data sets derived from lake sediment for Dry Lake, California and Crystal Lake, Illinois provide a detailed archive of landscape response to climate events. Climate sensitive proxies have been recorded to discern levels of precipitation, influx of glacial or locally derived sediments, and levels of soil maturation.

For Crystal Lake, the observed proxies varied with the GISP2 $\delta^{18}O$ curve with a noticeable multi-century lag attributed to mid-continental buffering and proximity to the receding glaciers. The changes in phosphorus and organic carbon were in sync with changes in pollen types as was seen by Gonzales and Grimm (2009). These combined proxies delineate late Pleistocene climate changes including the Younger Dryas stadial and provide a continuous record of progressive soil development.

The Dry Lake data curves display early soil development as temperatures increased after the Younger Dryas cooling event. The onset of the 8.2 kyr event showed a resetting of soil development with decreases in phosphorus concentration and organic carbon as the climate returned to glacial conditions. Soil development resumed with warming temperatures and more stable climate. These changes were corroborated by the GISP2 ice core data as well as the research performed earlier by Bird and Kirby (2006).

Further research for both sites would include much better resolution during the events - sampling every centimeter instead of multi-centimeter sampling - to offer better understanding of geochemical cycling within the events. The coring of additional sites in the region would provide samples of corresponding time frames so as to compare the results side by side where the severity of the cooling events, and the recovery times could be observed over a distance.

Table 1. Trace element data for Dry Lake samples. Carbon isotope dates in bold; (*) denotes lost samples.

Depth	Age	TOC	Al		Ba		Ca		Fe		K		Mg		Mn		Na	
cm	ybp	%	µg/g	± %error	µg/g	± %error	µg/g	± %error	µg/g	± %error	µg/g	± %error	µg/g	± %error	µg/g	± %error	µg/g	± %error
307	6925	2.2	83115	1.0	842	2.0	13786	0.9	60323	1.6	12044	0.6	4650	1.3	2068	1.4	22656	1.1
311	**6960**	4.0	89123	1.6	956	1.0	15354	2.5	49145	0.7	9715	1.0	8143	1.8	2265	0.6	17129	0.2
316	7004	1.5	138668	3.2	975	1.3	17217	3.1	76256	2.1	12457	0.6	18830	1.5	1748	1.7	21486	2.5
321	7047	1.5	80893	1.2	998	2.8	10220	3.7	45728	0.8	12081	1.4	7284	1.6	1485	0.7	16961	2.9
326	7091	1.7	122391	2.0	915	2.0	15203	1.7	71091	1.0	12399	1.9	13933	1.7	1891	2.9	20573	3.6
331	7134	1.7	81003	1.0	1030	2.2	10482	2.2	47997	3.0	12063	5.7	7451	2.2	1579	1.7	17239	4.2
337	7187	1.7	120831	3.4	968	4.0	13645	2.4	64852	1.5	11783	1.0	10850	2.5	1551	2.7	20018	2.3
344	7248	2.0	79129	1.9	928	2.0	11033	1.3	44750	1.4	10294	1.9	6769	1.6	1922	2.5	18156	3.4
349	7291	1.5	116280	5.5	963	1.8	15703	2.4	65386	2.3	13403	2.7	14440	2.7	1998	1.9	21244	1.0
354	7335	1.8	93382	1.5	887	2.0	11725	1.4	50014	1.5	10470	4.4	10101	0.8	1554	0.7	18270	3.8
364	7422	4.0	80769	1.1	1164	2.0	11606	1.5	36853	1.0	11992	3.6	8733	1.7	2613	0.8	14472	1.0
369	7466	1.4	110417	0.8	906	1.7	14070	2.1	52420	1.4	11918	1.4	13733	1.9	1005	1.4	20397	2.2
374	7509	1.3	121374	1.4	959	4.0	13651	2.5	71800	1.3	7565	1.5	15440	3.1	1430	2.4	21155	1.6
377	7536	1.5	64142	1.3	969	2.1	8679	0.7	30954	0.4	11236	2.1	5931	0.5	1277	1.4	15522	0.4
382	7579	1.5	147236	1.6	1002	1.8	16424	2.0	78515	1.9	13450	0.4	17888	1.3	1306	1.3	25048	1.1
387	7623	2.4	82678	0.8	1003	0.8	9259	1.0	56389	1.8	10756	3.3	7149	1.4	1500	0.9	14769	5.0
392	7666	3.5	135221	1.9	1072	3.3	12176	1.6	52238	0.5	12870	0.4	14658	2.5	1864	2.1	17443	4.7
397	**7710**	2.0	90511	2.0	1042	2.0	11219	2.6	44735	1.0	11683	2.2	11594	1.0	1172	0.1	17235	4.3
402	7715	3.4	136049	3.0	951	1.6	18794	2.6	70960	1.4	12058	2.1	19120	2.3	1445	1.0	22875	3.0
407	7720	1.5	98434	2.0	1110	2.1	11402	2.6	50871	1.3	12654	4.8	10676	1.4	1359	2.2	19754	0.7
412	7725	2.5	118256	2.7	979	2.1	13044	3.1	67203	2.3	11600	1.3	13290	2.3	1404	3.5	15943	2.0
417	7730	1.0	96307	1.3	910	2.2	14386	1.3	35365	1.5	11397	3.1	8104	1.5	786	1.0	30364	1.6
422	7734	3.5	100961	2.4	1136	1.5	15288	1.4	52518	1.0	15506	6.5	14566	2.6	1568	2.0	21773	0.6
427	7739	0.9	73072	2.9	1154	2.0	8462	0.7	33891	3.0	14542	2.0	6182	2.1	918	2.1	19851	1.3
469	7780	1.8	80523	2.4	874	2.3	8893	1.8	42553	2.4	10705	2.7	6477	2.2	1177	1.1	17233	3.7
474	7785	0.9	130382	1.1	1046	2.3	14841	1.9	51395	1.1	14423	0.8	12532	1.5	1306	0.8	25441	1.2
479	7790	1.6	76365	3.0	1012	0.8	9576	3.6	47818	2.8	12312	1.8	5926	4.0	1109	1.7	18298	2.7
484	7795	1.7	88546	0.7	731	1.6	11231	1.5	44532	2.1	10244	1.8	8060	0.4	1032	1.9	20039	2.6
489	**7800**	1.5	77511	1.3	899	2.4	10274	0.5	37004	2.9	10967	1.7	5834	1.3	1220	1.3	19658	4.5
494	7893	2.7	123735	1.5	1049	2.3	13941	3.5	56786	1.7	13395	0.5	12572	1.8	1618	1.5	19139	1.9

Table 1 continued.

Depth	Age	TOC	Al		Ba		Ca		Fe		K		Mg		Mn		Na	
cm	ybp	%	µg/g ±	%error	µg/g ±	%error	µg/g ±	%error	µg/g ±	%error	µg/g ±	%error	µg/g ±	%error	µg/g ±	%error	µg/g ±	%error
503	**8060**	2.0	92692	3.3	929	0.5	9552	2.0	41554	2.9	11260	2.9	10130	2.0	1281	2.4	17040	1.0
508	8064	2.4	116190	1.2	1031	2.9	16443	1.0	54971	0.4	13258	1.2	12260	0.7	1403	2.2	22823	3.4
513	8069	3.8	75008	0.2	998	2.5	11012	1.1	43096	0.8	11242	3.7	5218	4.0	1665	3.1	17708	3.5
518	8073	4.5	110066	2.7	1008	4.3	17226	2.6	64917	0.8	12974	1.0	12944	3.2	1565	0.9	23053	2.5
523	8077	3.0	84467	0.5	*	*	10366	2.4	37423	0.9	*	*	7497	2.6	1135	7.1	20069	4.0
528	8081	1.1	87219	0.7	928	1.6	11378	1.1	43909	4.4	13965	2.1	9579	0.8	735	1.5	15027	33.8
532	8085	0.7	105609	2.4	890	2.1	14224	1.2	37250	1.4	14030	15.2	10204	3.2	795	1.7	30367	0.7
537	8089	0.8	71656	1.9	904	1.8	10752	0.3	29174	1.5	11549	0.5	4674	2.4	882	3.3	25811	0.6
542	8093	0.6	90580	1.6	1297	1.5	13532	1.6	31714	1.4	17166	1.3	8189	3.6	1102	0.5	26706	7.9
598	8141	2.5	54896	1.3	981	1.4	7763	1.7	25730	1.6	10702	5.2	3765	2.0	1316	0.8	15863	1.0
603	8146	2.9	117491	4.3	859	2.7	15698	1.6	48657	1.4	11816	3.9	13642	1.9	1166	2.9	23970	1.7
608	**8150**	2.3	74848	1.2	980	4.3	11864	2.4	33049	0.4	11933	2.8	5729	3.8	1328	2.3	23452	1.2
613	8170	1.4	115157	1.8	1231	2.2	16749	2.2	41187	0.7	16859	2.2	12576	2.3	1419	2.2	30728	2.7
618	8189	5.3	75035	1.2	949	2.0	10582	1.3	41877	2.0	11636	4.3	5344	2.4	1712	2.3	15909	3.9
623	8209	3.2	109551	1.6	936	2.0	12411	2.0	58778	2.7	13607	0.9	13702	2.7	1306	1.1	17627	1.5
628	8228	2.2	83528	2.8	1473	2.6	8621	0.9	44957	0.7	18187	3.9	6945	1.6	1185	1.6	15366	1.3
635	8256	2.0	66816	1.1	880	1.9	9233	0.5	33423	2.5	11051	1.3	3927	3.7	890	1.4	18538	3.6
640	8275	2.2	125066	1.4	828	1.8	14073	2.2	58142	1.6	10832	23.7	13536	1.0	824	1.4	19941	1.9
646	8299	0.4	68466	2.8	923	4.0	8350	4.2	32136	1.7	11394	1.0	5181	2.2	523	2.9	18327	4.5
650	8314	0.4	87908	2.1	997	1.7	10673	1.2	40495	1.4	14079	0.5	10049	1.2	519	0.9	19810	0.5
656	8338	2.4	77460	2.0	961	3.6	9802	2.5	48655	1.6	12179	1.3	6518	1.6	1209	0.9	16833	4.5
660	8353	2.6	110991	2.7	984	3.3	11620	2.3	51370	0.4	13430	2.2	11960	1.5	1278	2.1	16584	1.2
665	8373	3.8	76677	1.0	1046	2.7	8845	1.6	39620	2.1	11614	0.0	6779	2.9	1370	3.1	14514	3.3
667	8381	0.4	61274	1.9	830	1.9	6440	2.8	32630	3.4	10271	2.1	5528	5.0	422	2.8	14680	5.0
670	8392	0.7	112110	2.3	775	1.9	11367	2.6	51826	2.6	11107	1.8	13333	1.3	465	1.7	19591	3.4
675	8412	1.3	62951	2.3	962	1.0	6921	3.3	36949	2.0	11716	1.6	4647	3.4	891	0.6	13359	4.9
680	8431	2.2	124418	2.0	1008	2.6	15747	1.6	48079	2.2	12942	2.8	12222	1.1	1255	1.0	27488	0.2
685	8451	3.2	72632	1.7	944	0.8	9219	1.9	39953	2.8	10902	0.4	4214	4.7	1399	0.6	16513	1.1
689	8467	2.5	100054	2.0	922	1.3	14813	1.2	46342	1.2	12898	2.5	11075	2.7	1197	1.7	22735	2.7
695	**8490**	6.6	59722	2.7	*	*	9477	1.2	31333	2.7	*	*	4705	2.4	1745	11.9	14443	2.2

Table 1 continued.

Depth	Age	TOC	Al		Ba		Ca		Fe		K		Mg		Mn		Na	
cm	ybp	%	µg/g	± %error	µg/g	± %error	µg/g	± %error	µg/g	± %error	µg/g	± %error	µg/g	± %error	µg/g	± %error	µg/g	± %error
700	8501	14.3	109732	2.6	970	1.4	17222	1.6	60513	3.3	12145	4.0	10967	3.7	2189	0.7	20473	4.7
705	8511	10.2	70462	0.3	1006	2.5	12018	1.1	40746	2.1	11835	2.2	4831	2.2	1314	0.8	14270	2.6
710	8522	8.5	133710	3.2	898	2.6	16010	1.7	70205	1.8	12299	1.9	17391	3.3	1599	2.4	21133	0.8
715	8533	3.8	65773	0.8	1010	2.3	10305	1.8	34426	0.7	12641	2.7	4046	2.0	1221	1.1	19321	0.8
720	8554	3.0	69351	0.7	1122	0.4	6987	1.4	26284	1.2	12333	4.2	5787	2.0	1125	0.9	13033	1.4
730	8565	2.6	118230	1.2	1018	2.2	15721	2.1	50801	0.7	14680	1.0	10498	2.4	1303	1.0	30967	0.5
734	8574	2.1	132867	0.8	1002	1.7	15204	2.1	54496	1.1	12948	1.4	11143	1.9	1270	0.7	30391	2.6
740	8586	3.4	125079	1.4	771	1.7	14651	2.5	52720	1.6	10610	1.0	11207	1.3	952	1.1	27544	1.4
745	8597	3.2	73128	0.6	1101	3.6	10257	1.6	27223	2.6	11561	1.1	3527	1.8	1865	1.9	23815	0.9
750	8608	1.6	106760	2.5	875	2.1	14669	2.1	29621	0.6	11684	0.5	7178	1.1	677	1.6	36801	1.4
755	8619	2.4	114254	2.3	1053	1.8	15698	2.4	47971	1.7	13771	1.3	5723	2.1	1031	2.7	34810	1.0
760	8629	3.4	137113	2.0	1041	1.6	15328	2.7	47908	2.6	14010	1.7	10309	1.3	1272	0.8	29528	2.9
765	8640	5.0	65065	0.2	927	0.6	9017	2.2	25111	2.4	10975	2.8	3668	2.2	1183	0.9	18697	1.1
770	8651	0.2	131660	1.8	1186	3.5	15893	2.9	19761	1.8	13358	0.3	5107	2.0	512	3.0	42113	1.0
787	8687	0.3	71716	1.8	1103	0.9	9054	2.7	11393	1.7	11516	0.6	2458	2.1	528	2.9	24601	2.5
792	8698	0.6	110333	1.2	1191	1.1	15187	2.5	18183	0.8	14188	0.2	4632	1.2	558	1.1	40547	1.7
797	8709	4.8	75578	1.2	901	2.0	11099	1.3	31239	1.4	11451	0.5	5515	2.7	1286	2.4	21105	2.4
807	**8730**	5.2	75448	1.6	846	2.0	9921	1.9	38098	3.3	10632	1.2	3757	2.3	1380	0.2	16597	1.7
813	8758	5.8	124895	3.2	817	1.8	14601	2.4	71887	1.9	11158	0.7	13627	0.9	1650	2.2	20985	1.2
817	8777	1.3	40903	1.8	1163	1.6	4549	1.6	10475	3.0	12207	3.6	1454	7.3	860	3.1	12548	1.7
822	8800	1.4	117281	1.1	1130	1.6	16935	0.8	50212	1.6	11283	0.6	13549	2.9	1396	2.2	34955	0.3
827	8823	2.9	76073	2.2	864	1.8	10911	1.2	43647	0.6	11189	3.9	5543	0.4	1474	1.3	19949	1.7
832	8847	3.7	96627	2.8	735	1.8	12060	2.8	54162	2.1	10606	2.9	9054	2.8	1214	2.0	21293	0.4
837	**8870**	15.2	90721	1.5	938	1.1	15169	2.3	50358	2.3	9816	2.0	6675	2.0	2588	2.4	15856	0.1
842	8893	5.3	144861	1.3	869	0.8	21022	1.3	62947	1.0	11129	2.4	16536	1.0	1413	1.8	36211	3.7

Table 1 continued.

Depth	Age	P		S		Sr		Ti		Zn		P occluded		P organic		P mineral	
cm	ybp	µg/g	± %error	µg/g	± %error	µg/g	± %error	µg/g	± %error	µg/g	± %error	µg/g	± %error	µg/g	± %error	µg/g	± %error
307	6925	1774	2.6	518	5.1	307	1.4	5825	2.2	244	1.7	790	1.6	93	1.6	156	3.0
311	**6960**	2533	4.5	1050	7.5	342	3.0	5167	1.8	305	1.0	923	2.5	143	1.2	226	4.0
316	7004	1899	0.9	598	8.5	318	1.7	7277	1.9	242	1.4	854	1.8	103	1.9	224	3.1
321	7047	1674	0.8	756	16.9	265	1.5	4523	0.9	211	1.2	756	2.9	102	0.6	190	3.2
326	7091	2181	2.2	652	7.2	301	0.9	6634	0.7	261	1.0	1132	2.5	126	0.6	178	2.4
331	7134	2320	3.3	1187	4.4	313	2.9	4841	0.9	296	1.5	658	2.8	126	1.2	193	2.0
337	7187	1699	4.8	760	14.1	298	3.0	6093	2.5	262	1.0	488	2.1	116	1.5	151	1.3
344	7248	2005	3.3	1099	2.2	276	1.7	4390	1.5	251	1.6	614	4.8	119	0.6	157	3.2
349	7291	1941	2.3	635	10.8	305	1.8	6207	2.1	250	2.1	654	3.2	105	0.7	183	1.4
354	7335	1920	3.4	1002	6.0	265	2.2	4875	2.2	233	2.5	708	1.2	112	0.6	184	0.6
364	7422	2127	0.3	1081	6.1	360	1.7	3851	1.1	322	1.8	757	1.4	148	0.8	195	2.0
369	7466	1249	0.6	517	9.8	273	1.5	5379	1.1	217	1.2	353	8.2	102	1.3	212	2.8
374	7509	1996	4.2	609	15.0	267	2.2	6020	2.0	210	1.8	736	2.5	87	1.9	194	5.5
377	7536	1643	1.1	926	4.6	292	2.4	3431	0.6	243	1.0	367	7.3	92	0.5	210	4.0
382	7579	1697	5.4	511	3.7	243	1.4	7688	1.8	198	3.6	679	5.7	85	1.2	172	2.6
387	7623	2391	2.9	912	11.3	252	1.9	4311	1.3	221	0.3	1377	1.5	115	0.8	158	5.6
392	7666	1842	3.0	912	8.1	314	2.5	7400	1.4	410	0.4	431	4.3	155	0.9	150	1.8
397	**7710**	1397	1.5	1155	5.7	297	1.5	4909	1.1	261	0.9	261	2.7	114	1.7	209	5.1
402	7715	1276	3.4	1187	3.8	302	2.4	6764	2.4	223	2.5	450	9.6	90	1.5	178	5.7
407	7720	1604	1.3	1076	12.5	321	1.1	4631	2.0	244	2.1	491	1.8	86	2.1	191	8.2
412	7725	1603	2.4	769	6.7	276	2.0	6794	2.4	278	1.1	470	8.5	149	0.9	174	3.8
417	7730	789	3.9	1001	10.6	308	1.9	3471	1.0	139	2.2	172	10.5	33	0.6	156	5.7
422	7734	1200	2.4	862	7.5	337	2.1	5770	1.7	223	1.7	241	8.3	72	2.0	149	3.0
427	7739	947	2.0	890	6.6	270	1.5	3332	2.1	156	1.1	183	6.2	36	2.0	174	5.0
469	7780	1207	1.7	1147	2.1	278	2.3	3936	0.9	227	1.2	294	9.0	88	1.6	158	2.9
474	7785	1553	2.8	754	7.4	340	1.2	5860	0.7	244	0.4	492	2.2	90	2.3	186	3.2
479	7790	1238	0.7	1030	13.7	297	0.7	3934	1.8	193	1.7	502	1.7	61	2.6	168	3.5
484	7795	997	1.5	476	1.2	255	2.3	4778	1.9	199	2.9	277	9.8	90	0.6	181	3.2
489	**7800**	1186	2.1	984	13.7	318	2.6	3781	0.1	221	1.3	346	8.0	77	2.3	184	5.3
494	7893	1518	0.8	1683	6.8	402	3.0	5608	1.5	329	1.5	312	17.2	100	3.0	146	8.6

Table 1 continued.

Depth	Age	P		S		Sr		Ti		Zn		P occluded		P organic		P mineral	
cm	ybp	µg/g	± %error	µg/g	± %error	µg/g	± %error	µg/g	± %error	µg/g	± %error	µg/g	± %error	µg/g	± %error	µg/g	± %error
503	**8060**	1284	2.1	1457	8.2	326	1.2	3957	2.6	252	1.6	256	13.4	93	1.4	170	8.9
508	8064	1411	2.1	1407	9.1	355	2.1	6063	2.4	276	3.1	413	1.6	79	0.9	175	1.1
513	8069	1681	0.9	2931	8.4	342	2.0	4553	0.6	315	1.9	492	6.3	92	0.7	175	2.0
518	8073	1419	1.9	3451	3.1	333	1.5	5967	0.4	248	1.6	405	0.4	65	1.5	190	6.1
523	8077	1283	0.8	2238	4.8	*	*	3719	1.6	175	2.8	390	2.8	44	2.6	211	3.3
528	8081	998	0.8	1086	3.4	227	2.0	4854	0.7	121	3.2	228	8.1	42	3.2	202	1.8
532	8085	940	4.5	900	3.6	303	2.4	4301	0.6	150	3.7	255	10.7	28	7.3	155	3.4
537	8089	849	3.3	1716	7.4	324	1.3	3091	2.5	149	0.6	287	10.9	26	1.9	161	4.2
542	8093	1306	3.1	1013	11.9	445	1.8	3760	2.2	157	0.7	270	13.4	31	7.8	191	8.6
598	8141	1411	2.3	1759	2.9	349	4.9	2679	1.5	241	0.2	312	9.8	65	0.9	148	6.4
603	8146	1259	1.7	1242	9.7	297	3.2	5157	0.8	193	1.9	296	6.4	46	3.1	220	1.4
608	**8150**	1432	2.5	1924	5.3	351	1.7	3380	1.0	193	1.7	247	5.2	49	1.3	201	2.5
613	8170	1407	2.1	939	15.9	436	2.9	4374	1.4	211	1.3	223	9.2	41	3.8	170	3.4
618	8189	1653	2.9	2424	5.2	317	1.4	4339	0.8	329	1.8	414	2.7	122	0.8	168	3.2
623	8209	1363	3.5	956	9.6	274	3.1	5616	1.8	246	2.8	358	3.8	100	1.3	186	1.1
628	8228	1287	3.6	1427	4.6	244	1.4	4908	0.8	194	1.8	314	8.0	51	2.4	137	3.5
635	8256	1030	1.8	1166	11.8	251	1.3	3470	0.9	169	0.2	221	6.9	60	1.1	163	5.5
640	8275	936	3.9	609	5.4	190	2.3	6365	2.1	157	1.0	317	9.0	62	1.4	158	2.5
646	8299	941	2.1	872	5.4	242	2.4	3224	1.7	96	1.8	144	20.0	19	6.9	138	2.9
650	8314	798	3.4	429	21.6	221	2.0	4872	1.2	85	3.9	156	5.6	26	4.0	141	6.0
656	8338	1269	1.2	1127	3.2	234	1.8	5058	0.6	206	0.6	326	4.8	88	0.7	171	1.2
660	8353	1627	3.1	868	3.8	274	2.2	5805	0.9	246	2.5	426	4.8	112	1.3	162	5.1
665	8373	2103	4.1	1322	6.8	288	1.1	4277	0.8	254	1.0	1060	1.7	131	0.3	224	1.6
667	8381	726	1.7	802	13.9	187	3.9	2981	1.7	86	1.4	176	18.7	18	10.9	160	5.1
670	8392	687	3.6	434	10.5	172	1.0	5275	2.6	92	1.5	165	9.9	34	6.2	123	10.2
675	8412	1031	1.4	1001	18.4	238	2.8	3546	2.1	151	0.9	299	16.1	52	1.2	150	5.4
680	8431	1545	1.4	627	20.3	381	0.9	4934	2.2	239	1.0	704	6.1	91	0.7	231	1.0
685	8451	1618	2.0	1174	10.5	365	1.6	3794	2.3	278	0.5	168	6.7	119	0.9	189	4.1
689	8467	1480	1.9	702	9.6	364	2.2	4919	0.3	234	0.6	439	5.5	89	0.7	200	4.5
695	**8490**	2503	3.2	2449	4.1	*	*	3143	1.3	312	2.8	811	3.6	98	0.1	211	5.4

Table 1 continued.

Depth	Age	P		S		Sr		Ti		Zn		P occluded		P organic		P mineral	
cm	ybp	µg/g	± %error	µg/g	± %error	µg/g	± %error	µg/g	± %error	µg/g	± %error	µg/g	± %error	µg/g	± %error	µg/g	± %error
700	8501	2969	1.0	3033	3.3	388	1.8	5373	1.7	338	0.4	1070	4.4	118	1.3	194	2.2
705	8511	1885	1.9	1428	9.6	307	1.9	3916	1.8	193	1.2	749	7.3	115	0.9	191	3.8
710	8522	2601	1.2	1980	2.5	283	2.5	6345	2.5	257	2.3	847	2.5	127	0.7	203	1.8
715	8533	1368	2.9	1297	4.3	346	0.5	3488	1.4	254	0.2	583	3.1	71	0.8	195	3.2
720	8554	1632	3.4	1094	2.7	404	1.8	2618	1.8	208	1.6	427	5.4	106	1.5	180	2.6
730	8565	1472	1.9	821	6.0	357	2.2	5559	0.7	234	1.9	478	3.0	78	2.2	211	4.1
734	8574	1932	2.1	813	12.6	336	1.4	5818	1.5	219	1.3	320	7.0	74	1.4	201	3.2
740	8586	1583	5.5	781	10.3	251	1.9	5216	1.7	178	2.7	632	1.2	102	0.9	234	1.3
745	8597	2946	3.5	2531	4.9	427	3.3	2868	1.4	344	2.6	524	2.6	64	1.1	218	2.3
750	8608	899	1.5	522	15.2	334	1.9	3036	0.5	124	2.7	385	2.4	36	4.6	151	8.9
755	8619	1316	3.3	692	15.8	366	2.7	4843	2.9	173	0.2	393	3.7	59	1.6	170	4.6
760	8629	1634	1.9	852	3.9	404	1.6	4711	1.1	277	0.5	350	3.7	106	0.9	205	1.4
765	8640	1237	3.0	1071	6.7	364	2.3	2391	2.7	200	1.3	458	9.2	55	2.5	164	4.1
770	8651	689	2.8	451	15.2	491	2.3	1905	1.5	108	3.3	170	7.7	13	5.9	129	7.7
787	8687	749	2.4	688	4.3	444	3.0	1163	2.3	108	1.2	287	7.4	11	13.0	168	3.4
792	8698	630	2.8	379	11.1	472	2.2	1969	0.3	113	1.7	223	6.0	15	15.2	130	2.4
797	8709	1320	1.2	1278	5.4	344	1.6	3214	0.7	199	1.3	404	5.6	59	0.9	183	2.2
807	**8730**	1372	2.7	1306	9.2	287	2.0	3821	2.4	227	0.9	413	5.2	100	0.3	154	2.8
813	8758	2169	0.4	1402	5.3	257	1.3	6735	2.3	244	2.8	637	2.2	132	0.2	193	3.1
817	8777	987	4.3	1002	11.2	476	4.1	921	3.6	173	2.6	233	8.3	42	3.3	139	6.7
822	8800	1442	2.5	702	9.1	398	1.6	5044	1.8	215	2.1	238	0.5	43	2.4	216	2.8
827	8823	1702	3.4	1141	5.5	308	1.7	4579	1.3	234	0.9	508	4.9	90	1.7	265	1.3
832	8847	1575	3.9	711	3.1	259	2.7	5522	2.1	215	1.9	366	5.7	83	1.1	208	2.3
837	**8870**	3474	2.7	3981	6.7	334	2.0	4568	1.2	294	1.2	871	7.5	136	0.7	211	1.9
842	8893	1856	3.0	982	3.4	311	2.7	7094	1.2	222	0.2	781	2.5	91	0.8	242	3.5

Table 2. Trace element data for Crystal Lake samples. Carbon isotope dates in bold; (*) denotes lost samples.

Depth	Age	TOC	Al		Ba		Ca		Fe		K		Mg		Mn	
cm	ybp	%	µg/g	± %error	µg/g	± %error	µg/g	± %error	µg/g	± %error	µg/g	± %error	µg/g	± %error	µg/g	± %error
1762	8947	3.21	14364	1.2	514.5	0.4	334308	1.2	44220	2.0	3132.5	3.9	12177	3.2	1072	0.5
1763	8970	3.35	9557	1.7	456.2	1.5	293834	0.1	36982	1.0	2409.1	0.8	11252	2.5	964	1.1
1764	8993	3.18	4207	2.1	422.8	1.4	365059	1.1	36258	0.6	1296.2	0.5	8360	0.4	610	0.5
1765	9015	3.61	3912	1.1	416.7	1.6	351053	0.6	36635	0.5	907.3	3.8	10397	1.6	833	0.4
1766	9038	3.34	4407	0.7	373.7	1.3	387754	1.9	37296	0.8	915.6	1.1	13227	2.1	971	2.4
1767	9060	3.03	3789	2.8	398.8	1.6	432760	2.0	36113	0.5	854.3	3.0	11226	1.9	890	1.2
1787	**9511**	3.40	4039	0.6	422.7	1.0	396261	1.8	50955	1.0	917.2	7.5	11723	1.9	1217	1.1
1795	9723	3.15	3438	2.2	494.6	1.7	411237	1.6	49116	1.3	754.6	5.3	11015	0.6	2053	2.6
1802	9908	5.17	3360	1.9	468.0	1.3	304182	0.3	93344	1.1	981.0	4.8	9289	1.3	4062	0.9
1806	10014	4.88	3656	1.1	457.4	0.5	279430	0.6	84272	1.0	829.0	3.3	9418	1.2	3325	0.6
1813	10199	3.44	4036	1.2	445.0	0.3	344329	1.9	58996	0.6	865.1	2.1	9318	1.7	2213	2.0
1819	10358	3.54	5227	3.3	471.8	0.6	374123	0.7	77888	0.6	1155.5	4.3	10303	2.9	2883	1.0
1847	11042	5.95	4088	2.5	503.5	0.6	385763	1.8	139812	1.7	945.1	0.8	10925	2.0	6294	1.5
1850	11109	5.78	3265	3.6	505.0	0.3	239859	0.3	166912	0.6	726.9	1.4	7061	1.0	7267	2.4
1854	11197	8.51	4143	3.7	534.3	1.1	254393	0.5	210639	1.2	966.5	2.7	7214	1.6	12130	1.2
1859	11307	6.63	3904	3.8	414.1	1.6	258600	0.6	242048	0.1	648.1	2.8	6664	2.3	9228	0.8
1863	11396	7.82	4055	2.5	458.9	1.2	306209	0.8	235682	1.5	858.9	5.1	7240	3.5	8157	0.6
1869	11504	7.27	3336	1.7	545.1	0.8	168792	2.6	341543	0.4	730.5	2.4	4657	1.2	22836	0.8
1876	11601	7.69	4051	1.6	458.8	1.4	168488	1.6	351937	1.6	815.2	5.6	4922	2.2	21565	0.5
1890	11796	7.76	2728	4.7	538.0	2.3	128547	0.9	416359	0.2	604.7	3.0	3560	0.9	31968	0.8
1897	11893	6.37	4276	0.9	550.7	1.3	239020	0.4	245759	0.5	1060.3	2.3	5380	2.1	20494	2.1
1905	12004	7.13	5925	1.8	482.0	1.3	179732	1.5	248292	0.7	1122.6	9.8	6470	3.0	27358	2.1
1911	12087	8.02	6330	1.1	523.5	1.9	196481	1.3	278586	0.4	1347.6	2.6	5987	2.8	20194	3.5
1939	12204	7.21	4145	1.4	547.1	1.5	187673	1.1	300248	1.8	1010.1	0.7	4562	0.9	25731	2.7
1965	12300	4.49	5698	3.1	538.4	1.3	325491	2.2	198998	1.5	1329.0	2.9	6084	2.1	10840	1.5
1975	12405	6.73	4468	3.6	424.0	2.7	173031	0.8	304349	0.3	807.5	4.7	4173	3.4	28449	2.3
1982	12521	6.81	4095	1.1	672.9	1.5	147174	1.0	346818	1.3	1075.1	4.4	3897	1.5	31983	0.7
1987	12604	6.86	2628	4.9	437.2	1.6	166965	3.2	455334	0.5	572.3	3.7	3324	2.9	18931	1.5
1991	12670	7.26	4073	4.9	534.9	1.4	145416	0.9	371191	0.5	771.3	3.1	4426	3.7	28497	3.1
1992	12686	7.40	4807	2.8	573.3	1.5	158745	1.5	493665	1.1	786.6	3.5	4038	0.8	26059	1.0

Table 2 continued.

Depth	Age	TOC	Al		Ba		Ca		Fe		K		Mg		Mn	
cm	ybp	%	µg/g	± %error	µg/g	± %error	µg/g	± %error	µg/g	± %error	µg/g	± %error	µg/g	± %error	µg/g	± %error
1993	12703	8.50	3633	1.9	571.6	0.7	123307	2.3	558948	0.6	802.2	1.3	3360	0.4	30238	2.7
1996	12719	5.24	11679	1.1	568.5	1.2	190155	2.2	248626	0.6	2360.4	3.0	6182	1.2	12248	2.9
1997	12769	4.88	9709	1.8	486.1	1.9	215296	1.5	222503	0.7	2059.7	3.5	7013	1.5	9189	0.3
1998	12786	3.89	6827	1.4	529.5	1.3	307934	0.5	193351	1.1	1654.2	1.2	7596	0.3	6215	0.8
1999	12802	4.81	5267	2.6	539.2	0.6	209631	2.0	218899	1.4	1420.1	2.0	6751	1.5	11967	0.2
2000	12819	5.52	5534	2.0	509.5	1.1	218281	0.2	328989	0.8	1152.0	5.0	5564	2.8	15109	3.0
2001	12835	4.58	5870	1.6	271.9	31.4	272440	0.9	264845	0.9	*	*	6865	2.7	12865	0.7
2002	12852	4.67	5065	4.3	471.9	1.6	245703	1.1	216643	1.3	1028.0	1.0	6450	1.1	12015	1.2
2003	12868	4.90	6126	2.6	510.4	1.7	323876	0.8	305774	0.3	1120.9	2.7	7586	3.3	15678	2.0
2004	**12885**	5.20	4149	2.8	544.9	1.8	231591	1.0	311287	1.1	978.2	5.7	5659	3.1	13901	1.7
2005	12903	5.21	4601	1.7	463.7	0.5	247952	1.5	312919	0.5	977.4	4.3	5207	2.5	12537	1.2
2006	12920	4.16	4411	0.4	513.5	0.4	223847	1.3	214873	0.4	1057.6	5.5	6132	2.0	8183	0.4
2007	12938	4.16	4741	0.7	529.7	0.6	251745	1.5	189919	0.6	1064.7	2.0	7025	1.7	9148	1.7
2008	12955	5.86	7028	2.1	457.3	1.7	162050	1.6	259424	1.2	752.1	3.2	5588	1.7	18727	1.4
2009	12973	4.99	6559	0.4	551.7	1.7	267679	1.1	297898	0.6	1281.3	1.5	6106	2.3	13485	2.0
2016	13095	4.99	6776	2.2	545.7	1.8	261296	1.6	323656	0.5	1289.2	1.1	7131	1.9	13503	2.2
2023	13214	4.92	5572	3.9	591.5	1.8	323075	2.0	333693	0.8	1246.2	5.2	6797	0.5	17735	2.5
2028	13280	6.27	9004	1.4	645.2	2.3	159241	0.8	352544	0.5	1584.2	3.9	6716	1.9	18065	2.5
2034	13353	6.04	6574	0.5	617.9	1.8	251017	1.9	485067	0.3	1386.6	3.9	5516	1.5	20572	1.3
2035	13365	7.18	7200	1.9	614.3	0.9	168959	1.1	395747	1.1	1284.6	5.1	5881	2.0	25510	1.3
2036	13377	7.93	5342	1.9	588.7	1.3	135256	2.0	514683	0.3	1036.1	7.0	4427	3.0	24668	3.3
2037	13389	8.70	5061	3.3	531.1	2.0	75278	1.0	323327	2.0	836.6	5.6	4168	1.5	28442	1.7
2038	**13401**	6.89	5547	1.2	574.0	0.6	191652	1.2	418899	0.6	1196.5	2.0	5458	2.4	17838	1.1
2039	13419	2.83	5043	2.6	486.3	1.5	302144	2.3	134745	1.7	1128.0	1.6	7752	1.8	3428	2.3
2043	13493	8.08	5814	1.7	588.6	1.4	99276	2.3	459338	1.5	1295.8	3.1	4393	0.2	24337	1.3
2059	13785	3.89	893	4.8	388.0	0.5	172636	1.2	198224	0.5	2142.6	2.1	464	56.3	3494	1.4
2066	13927	6.42	14172	1.5	592.0	2.0	110040	1.1	303932	0.9	3272.6	1.4	8200	3.1	11232	1.4
2067	13953	6.65	12915	2.0	565.3	1.7	117124	0.5	372207	0.4	2724.9	2.7	7353	2.8	15498	0.4
2068	13978	6.45	11258	1.3	560.0	2.1	108750	1.3	291916	1.2	2722.8	2.8	7650	0.9	12180	1.0
2069	14003	4.62	9668	2.3	466.0	1.1	231766	1.8	234831	1.0	1664.2	2.5	9024	3.0	10805	2.7

Table 2 continued.

Depth	Age	TOC	Al		Ba		Ca		Fe		K		Mg		Mn	
cm	ybp	%	µg/g	± %error	µg/g	± %error	µg/g	± %error	µg/g	± %error	µg/g	± %error	µg/g	± %error	µg/g	± %error
2071	14036	4.30	8917	2.7	537.9	1.6	187026	1.6	227354	1.1	2142.6	1.3	8024	3.8	12566	0.3
2072	14043	6.11	11477	1.5	591.5	1.8	164634	0.9	330529	1.2	2573.4	2.9	8219	1.6	17361	0.6
2073	14051	4.85	11181	3.2	363.6	1.1	256698	0.6	298346	2.1	1499.7	4.4	8040	2.2	15620	0.9
2075	14067	3.81	9616	2.8	512.9	1.5	258659	1.5	201950	1.0	1786.0	12.5	8901	1.8	15771	0.3
2076	14074	4.66	9020	3.2	495.6	0.7	278354	1.2	309547	1.1	1803.2	1.5	7799	2.2	12118	0.3
2077	14082	2.38	6905	1.1	466.9	0.9	268840	1.8	117568	1.2	1574.1	1.7	9576	0.7	4997	0.6
2079	14097	4.16	13024	4.8	513.5	1.2	125940	1.2	267789	1.1	4500.4	1.9	12467	1.3	13369	1.1
2080	**14105**	1.53	15413	0.5	550.5	2.5	160517	1.4	179570	0.6	4806.4	3.0	13392	1.2	5820	0.3
2082	**14140**	7.36	12294	1.5	509.9	1.7	85695	0.6	387240	0.4	2621.1	1.0	7611	1.8	15882	1.7
2089	14158	9.81	11709	0.6	593.7	0.5	148098	3.0	595783	0.7	2367.6	2.2	7514	1.7	28887	1.6
2096	14175	3.15	17737	1.1	564.7	0.8	265279	1.1	70525	0.7	4135.0	1.7	12777	3.0	3282	0.7
2107	14203	3.95	30942	1.1	752.3	3.4	226025	1.3	115512	1.3	6466.2	2.0	13255	1.4	3339	1.3
2115	**14434**	3.00	36169	0.3	700.3	1.3	173921	0.4	70650	0.8	7555.0	1.7	15584	1.7	1608	0.5
2126	14613	2.10	25543	1.4	601.8	1.1	246223	1.0	62054	0.7	5404.6	1.0	13245	1.1	1018	2.9
2137	14792	3.56	51149	4.1	861.3	0.9	89665	2.7	104620	2.0	9412.7	1.3	18298	2.8	2324	1.7
2143	**14890**	3.51	64221	0.6	731.8	1.0	92362	2.0	96264	1.5	8582.3	1.6	18698	3.7	1341	4.7
2152	15192	3.39	48819	0.7	924.8	2.5	91580	1.7	108723	0.8	10992.1	0.5	16987	2.1	1130	1.4
2158	15393	3.22	47960	1.2	1024.5	0.3	99322	0.8	78682	1.6	12353.1	0.6	17545	0.3	1020	1.4
2163	**15560**	2.44	47704	0.9	828.6	0.3	89380	0.5	75236	1.2	10069.3	0.4	17187	2.8	1106	0.8
2176	15631	2.28	32399	1.2	711.2	0.8	201327	1.4	64137	0.2	8273.4	0.6	19927	4.1	1237	3.4

Table 2 continued.

Depth	Age	Na		P		S		Ti		P occluded		P organic		P mineral	
cm	ybp	µg/g	± %error	µg/g	± %error	µg/g	± %error	µg/g	± %error	µg/g	± %error	µg/g	± %error	µg/g	± %error
1762	8947	4905	3.5	1410	2.0	12627	1.5	1579	0.6	1158	1.8	40.17	1.2	125	6.3
1763	8970	4105	2.0	1253	1.9	11635	12.6	1023	0.6	1245	1.6	31.41	5.9	121	4.4
1764	8993	3082	1.2	1317	1.9	10907	5.8	589	1.0	848	3.9	28.00	2.9	106	10.5
1765	9015	2924	3.4	1506	1.5	17548	1.5	505	1.0	1668	2.8	38.64	3.9	121	4.4
1766	9038	2428	2.4	1222	1.5	23009	3.4	401	1.5	1034	8.9	46.66	1.7	144	4.9
1767	9060	2584	3.5	1276	2.3	20390	1.8	418	1.3	1404	1.2	32.09	3.7	119	5.9
1787	**9511**	2896	1.1	1410	4.2	15498	8.7	415	0.8	1061	5.7	30.95	1.5	104	7.5
1795	9723	2913	6.0	1629	0.9	12358	5.5	318	1.0	1109	3.8	29.91	2.7	75	9.1
1802	9908	2869	2.2	1772	1.9	19988	2.4	455	1.4	1268	2.6	38.34	0.8	95	5.5
1806	10014	2419	1.5	1692	1.4	20867	5.6	356	0.5	945	4.8	49.03	1.8	95	12.5
1813	10199	4966	1.2	1345	0.7	11436	1.7	375	0.9	1165	1.3	57.45	1.4	83	3.4
1819	10358	3088	1.8	1466	1.4	10865	4.2	502	1.2	990	2.9	23.06	7.1	92	4.1
1847	11042	3206	2.4	2756	0.6	16522	11.5	392	0.3	1443	4.0	42.75	1.4	263	1.8
1850	11109	3030	4.2	3670	0.9	22275	3.7	357	0.8	2363	1.8	40.18	3.1	127	2.5
1854	11197	3271	2.8	4254	0.8	15988	2.4	405	0.6	2360	3.8	49.41	1.8	166	2.7
1859	11307	2412	4.1	3259	0.4	16397	2.7	331	0.3	2198	1.2	41.38	1.3	116	6.8
1863	11396	3318	1.1	3311	0.7	11464	5.8	395	0.9	2581	3.7	49.71	1.4	190	4.6
1869	11504	2749	1.1	7063	0.1	10418	5.1	372	1.1	1358	2.1	33.45	2.0	261	2.6
1876	11601	2360	4.0	5232	1.4	15902	10.8	422	1.2	3577	2.3	56.17	2.9	472	2.3
1890	11796	2566	4.6	9847	1.8	26935	0.9	330	1.7	1441	9.4	64.05	3.2	569	0.8
1897	11893	3267	0.3	4959	1.5	19285	3.1	480	1.1	3103	2.7	43.54	0.4	245	3.7
1905	12004	4627	5.7	5515	1.6	17174	3.2	573	1.3	3026	2.3	46.80	1.8	173	2.8
1911	12087	5181	2.0	5525	1.4	13220	1.4	696	1.2	3708	1.4	70.45	2.0	271	0.6
1939	12204	2747	4.4	5380	1.0	9787	5.9	455	0.8	3356	1.9	42.01	2.8	283	1.3
1965	12300	3106	1.5	3538	1.8	13566	5.7	630	1.5	1201	10.8	29.84	2.8	218	3.2
1975	12405	1830	4.7	5880	1.8	24589	3.9	423	1.8	3800	1.6	44.28	2.5	265	1.6
1982	12521	2961	1.3	9075	0.4	14389	2.4	521	1.4	4758	1.9	36.28	2.2	440	1.2
1987	12604	1958	6.7	8140	1.2	13118	3.6	294	0.1	4872	2.1	34.92	0.3	277	2.6
1991	12670	4235	3.3	4903	1.5	6261	5.6	378	0.8	2221	1.6	49.09	0.9	833	1.4
1992	12686	4486	2.1	7005	0.9	6296	5.4	385	1.4	3141	2.8	68.25	1.5	1000	0.7

Table 2 continued.

Depth	Age	Na		P		S		Ti		P occluded		P organic		P mineral	
cm	ybp	µg/g ±	%error	µg/g ±	%error	µg/g ±	%error	µg/g ±	%error	µg/g ±	%error	µg/g ±	%error	µg/g ±	%error
1993	12703	4723	2.9	6420	0.9	7956	9.8	376	0.4	1114	5.8	76.11	1.9	1216	0.5
1996	12719	6610	1.2	3545	0.6	9702	3.1	1126	0.9	2497	4.3	37.38	7.4	213	1.8
1997	12769	5575	2.0	3227	1.7	12448	7.0	1017	0.6	731	6.9	44.00	1.5	186	2.2
1998	12786	5440	1.3	2797	2.5	11512	5.0	847	0.8	736	9.3	32.28	1.0	190	2.5
1999	12802	5231	2.0	3464	0.9	12421	5.4	734	0.9	2400	3.0	29.88	9.1	265	1.6
2000	12819	5013	1.7	3519	1.6	9365	11.3	513	0.3	2078	3.7	31.08	2.5	241	2.3
2001	12835	*	*	2233	1.6	7901	7.3	413	2.0	2234	2.6	43.14	1.5	323	2.7
2002	12852	4226	0.3	2311	2.7	7759	2.6	463	0.6	1997	3.1	38.39	0.1	230	3.0
2003	12868	4758	1.3	2951	0.4	9817	5.5	531	1.1	2140	3.8	38.81	1.3	275	0.5
2004	**12885**	5054	0.5	3882	0.3	14889	9.1	457	0.5	2155	2.1	45.02	2.0	345	1.2
2005	12903	4277	1.7	2830	2.1	14663	4.2	423	0.7	2310	4.5	45.15	2.0	268	2.8
2006	12920	4790	1.0	2146	0.4	12392	3.8	470	0.6	886	11.2	33.77	3.4	177	4.5
2007	12938	4895	1.4	2321	0.5	13982	5.0	495	0.9	2413	1.6	38.77	2.8	243	2.5
2008	12955	5910	1.0	3106	3.4	10012	8.7	398	0.3	1347	6.5	36.14	3.8	312	2.5
2009	12973	8373	2.0	3418	0.5	10712	3.2	671	1.2	2245	1.3	35.73	4.3	254	2.5
2016	13095	5129	3.3	3052	2.6	17563	1.5	656	0.5	1791	0.6	33.45	6.0	195	3.4
2023	13214	5116	2.1	2854	1.1	12046	1.8	608	1.2	2100	1.5	36.46	5.2	289	2.2
2028	13280	6301	2.9	4521	0.9	12567	5.4	853	0.7	2443	1.8	47.62	0.6	340	2.2
2034	13353	5360	1.5	3132	1.4	16775	8.8	754	0.5	1056	4.8	59.33	1.3	373	2.2
2035	13365	4854	1.0	5353	0.6	13009	6.0	654	1.2	1976	4.2	56.18	2.0	817	0.6
2036	13377	4618	1.0	4445	0.5	11359	4.0	529	0.4	2145	3.5	72.63	0.5	837	1.1
2037	13389	4206	1.2	4164	1.6	17633	7.7	427	1.2	2352	2.4	81.64	2.2	1028	1.1
2038	**13401**	5213	0.3	3167	0.9	24482	4.4	551	0.7	1682	1.7	59.21	3.2	649	0.6
2039	13419	4744	1.9	1390	4.7	37990	3.4	507	2.2	1252	1.6	33.32	2.9	188	3.3
2043	13493	5740	2.5	4864	1.0	15167	4.0	646	1.0	1969	3.2	76.10	0.8	726	1.1
2059	13785	9747	0.6	1469	2.6	15361	3.9	989	0.8	1397	3.2	45.68	3.4	182	3.1
2066	13927	11109	2.2	2768	3.0	30700	4.6	1768	1.0	677	11.4	56.43	3.8	307	1.1
2067	13953	10115	0.7	2870	2.3	21220	3.8	1510	0.8	1409	2.9	76.84	1.7	426	2.2
2068	13978	9922	1.7	2896	0.6	20322	0.2	1560	1.4	1362	4.7	81.36	0.6	329	1.6
2069	14003	7888	1.2	1606	2.8	32244	6.7	927	1.3	1445	0.7	76.59	1.8	287	2.1

Table 2 continued.

Depth	Age	Na		P		S		Ti		P occluded		P organic		P mineral	
cm	ybp	µg/g	± %error	µg/g	± %error	µg/g	± %error	µg/g	± %error	µg/g	± %error	µg/g	± %error	µg/g	± %error
2071	14036	9064	0.5	2129	1.6	35264	1.7	1051	0.8	286	9.6	51.48	1.9	332	0.9
2072	14043	9408	1.4	2756	1.5	17908	6.5	1340	1.3	1679	4.3	44.35	2.3	374	0.9
2073	14051	4516	1.5	1178	1.9	27512	1.7	735	1.3	1431	8.0	73.90	1.3	299	2.0
2075	14067	7198	3.0	1694	1.0	48078	4.6	929	1.5	1294	4.0	45.70	2.7	227	3.3
2076	14074	7857	1.5	1766	1.7	42622	1.2	814	0.8	1429	2.0	44.15	1.4	254	1.5
2077	14082	7718	3.1	1041	3.7	49494	4.1	699	0.6	143	2.8	33.96	3.8	132	5.4
2079	14097	11270	2.2	2020	0.4	18696	1.9	1326	1.3	769	13.4	37.86	2.9	288	3.0
2080	**14105**	11862	0.5	1751	1.7	30392	1.3	1801	1.9	814	5.6	64.81	1.8	199	3.6
2082	**14140**	9676	0.8	2584	0.8	37334	2.1	1542	0.7	934	5.8	82.46	1.4	298	1.3
2089	14158	4577	1.5	3595	1.1	15426	3.2	1258	1.4	1508	0.8	88.22	1.4	789	0.5
2096	14175	5880	1.8	912	3.0	9232	6.3	1909	1.5	736	2.1	34.71	2.8	178	2.1
2107	14203	14159	1.6	1647	2.0	35132	3.8	4019	1.6	742	2.4	60.29	1.7	245	2.8
2115	**14434**	14325	1.4	1153	1.5	10709	5.7	3575	1.4	702	1.7	56.94	2.5	319	2.5
2126	14613	12008	1.2	1015	3.1	17245	5.5	2754	2.0	758	4.6	48.19	2.6	234	2.0
2137	14792	16502	1.0	1737	2.6	23129	0.2	5193	1.7	746	5.2	76.38	1.5	409	0.7
2143	**14890**	14504	0.9	1397	1.3	18165	6.2	4459	1.6	690	2.3	75.58	3.1	413	2.9
2152	15192	18716	1.0	1820	1.0	29806	3.1	6016	2.5	648	2.3	70.44	2.7	364	1.5
2158	15393	22069	2.7	1735	2.3	17972	3.7	6024	0.8	806	9.3	63.82	1.8	391	1.1
2163	**15560**	16801	1.8	1583	2.3	18518	3.0	5272	1.6	694	6.9	74.94	2.3	388	2.6
2176	15631	15693	2.4	1248	0.9	15500	4.2	4161	1.3	504	3.8	52.98	0.6	346	2.6

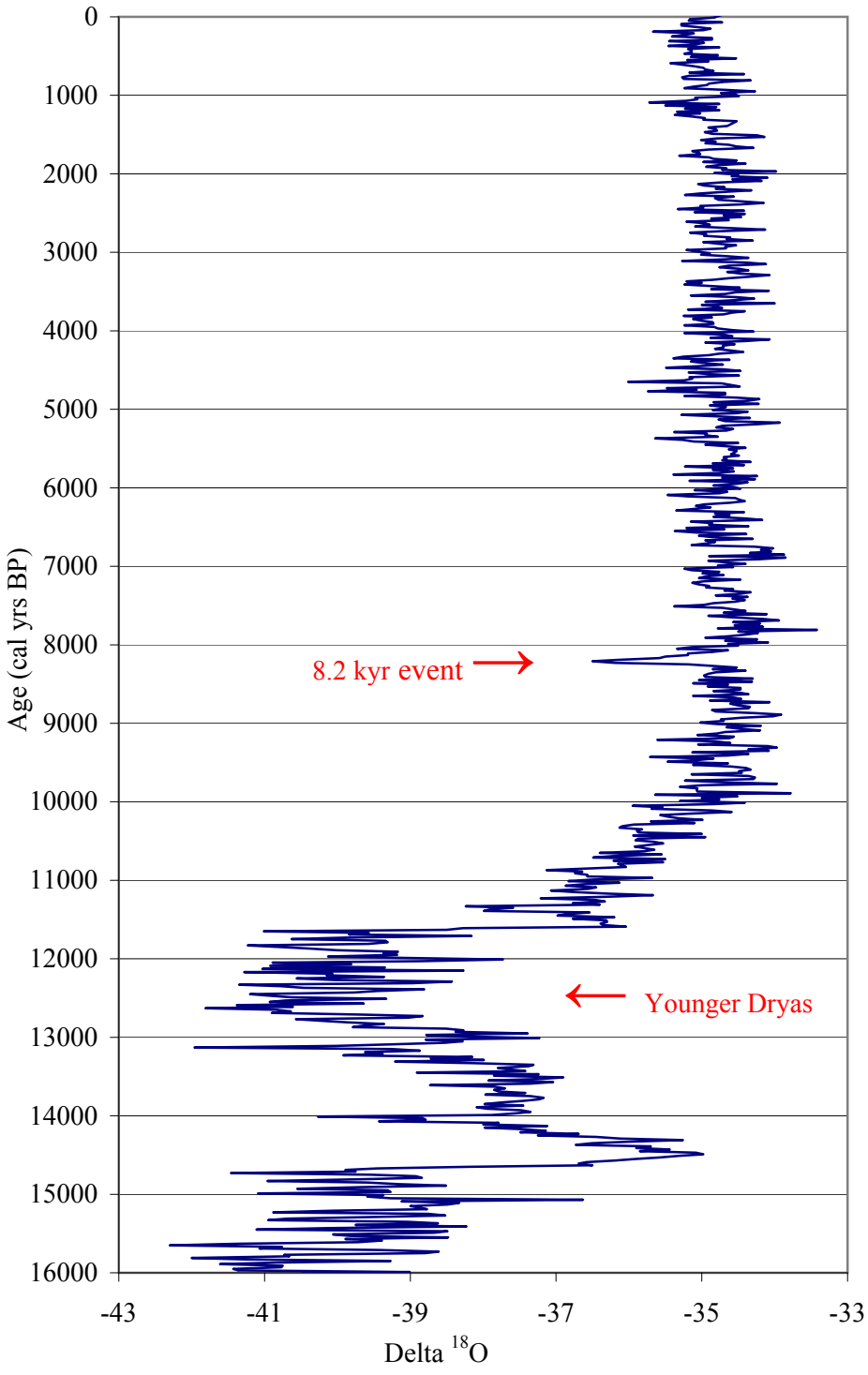

Figure 1. Late Pleistocene/Holocene climate changes as detected by the Greenland Ice Sheet (GISP2) delta 18 oxygen isotope data (Meese et al., 1994; Stuiver et al., 1995).

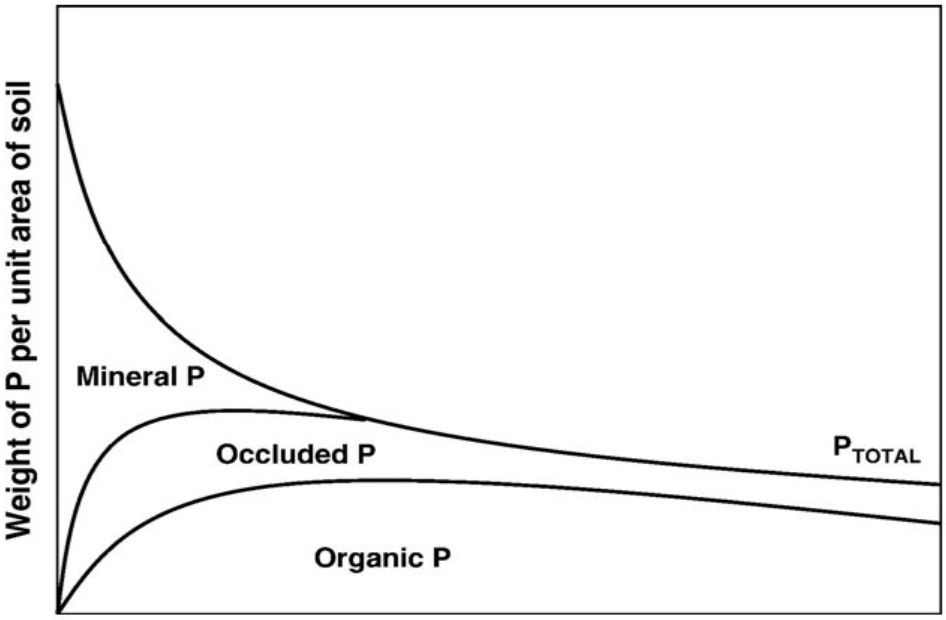

Figure 2. Geochemistry of soil phosphorus types over time (based on Walker and Sayers, 1976).

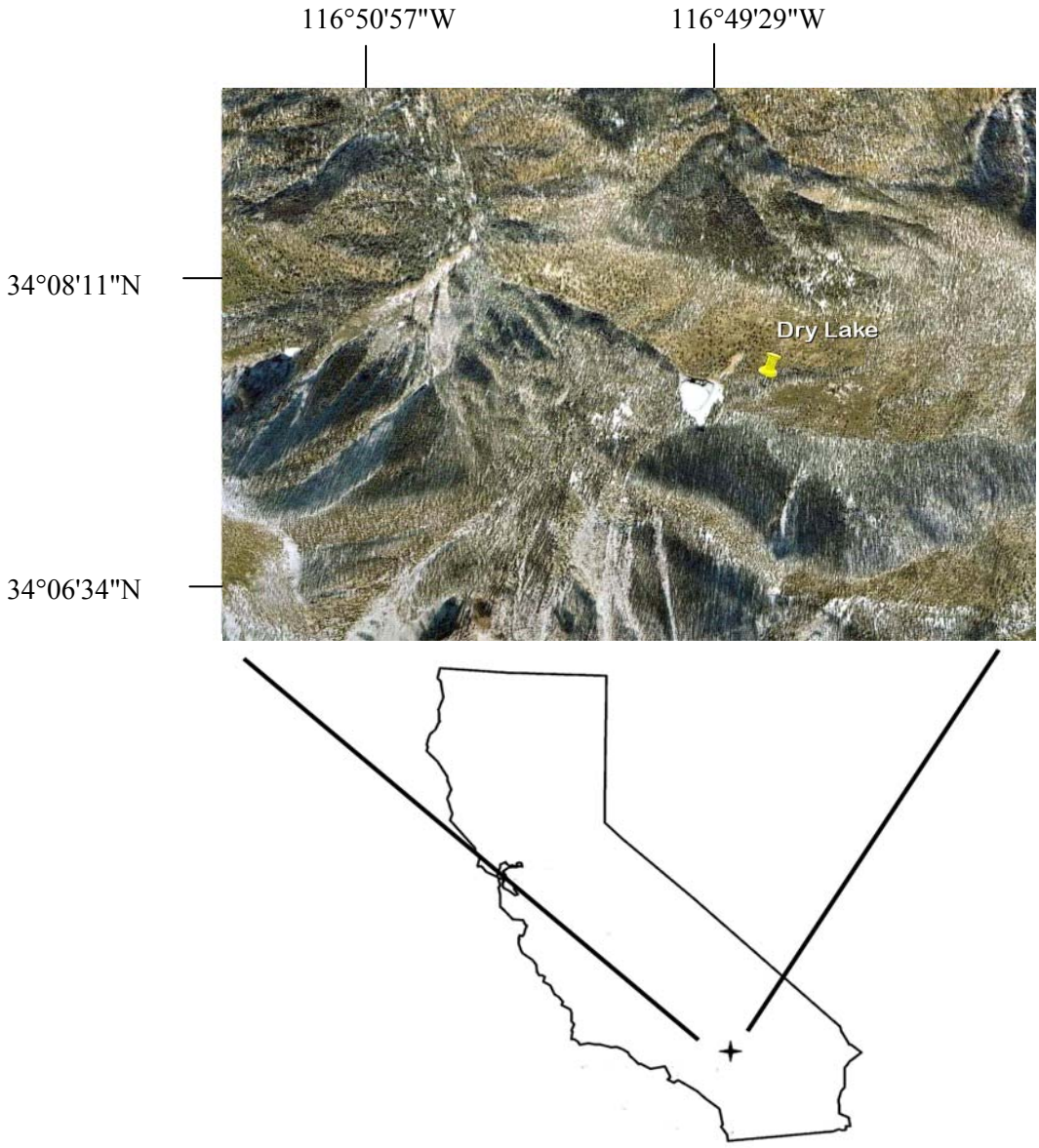

Figure 3. Dry Lake, CA

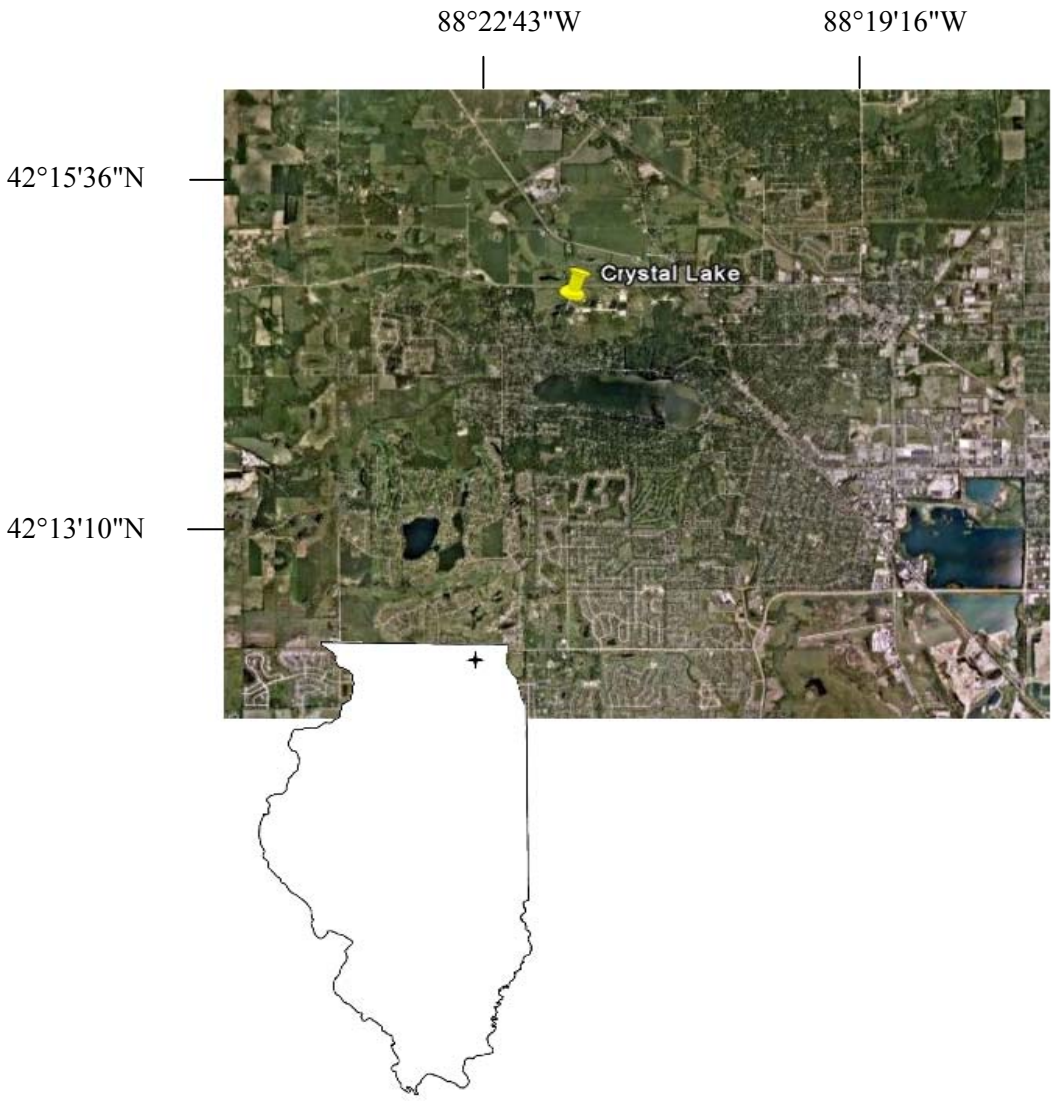

Figure 4. Crystal Lake, IL

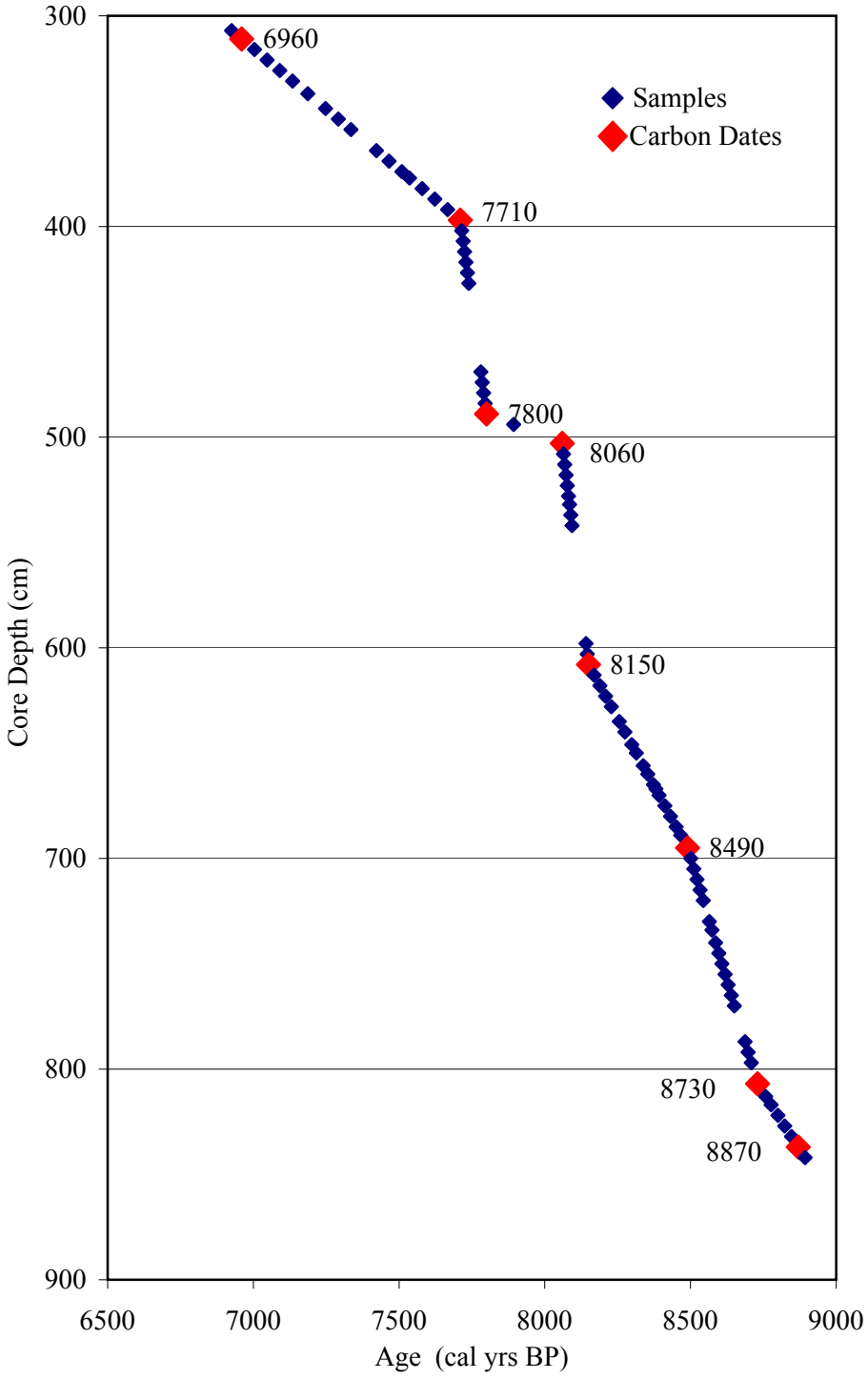

Figure 5. Dry Lake depth of core samples and carbon dates.

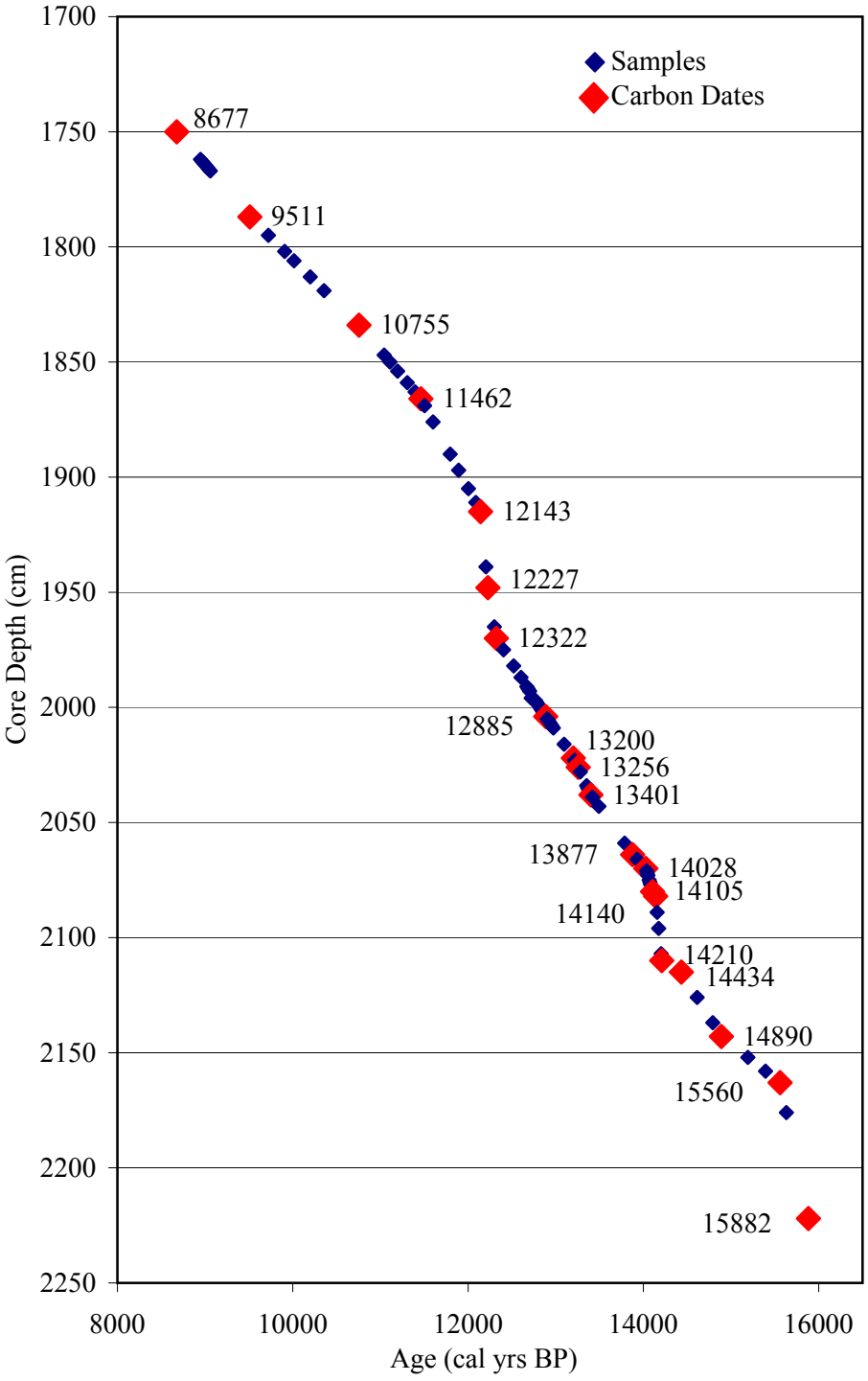

Figure 6. Crystal Lake depth of core samples and carbon dates.

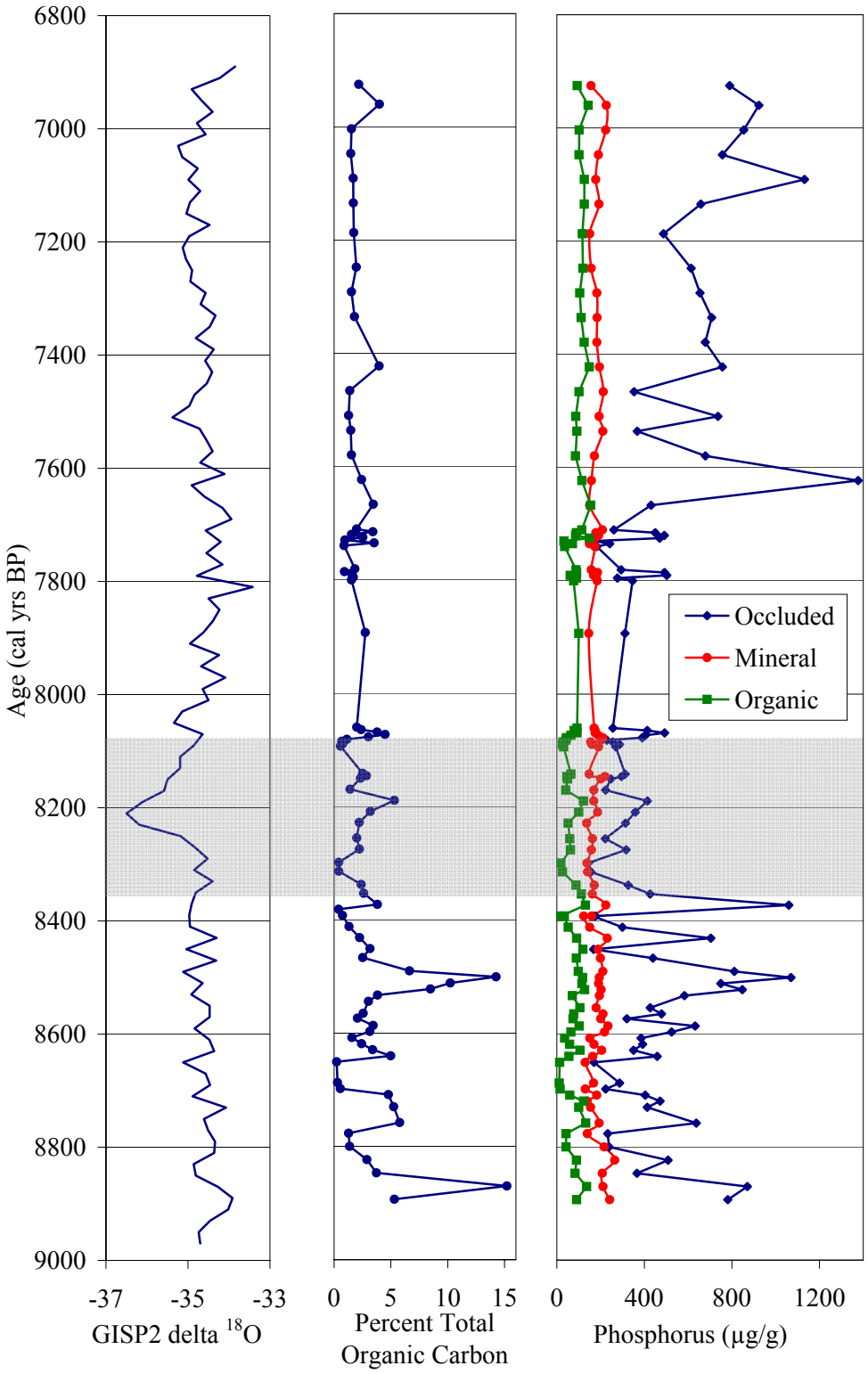

Figure 7. Dry Lake phosphorus concentration, percent total organic carbon, and GISP2 ice core data. The 8.2 kyr event is shaded in grey.

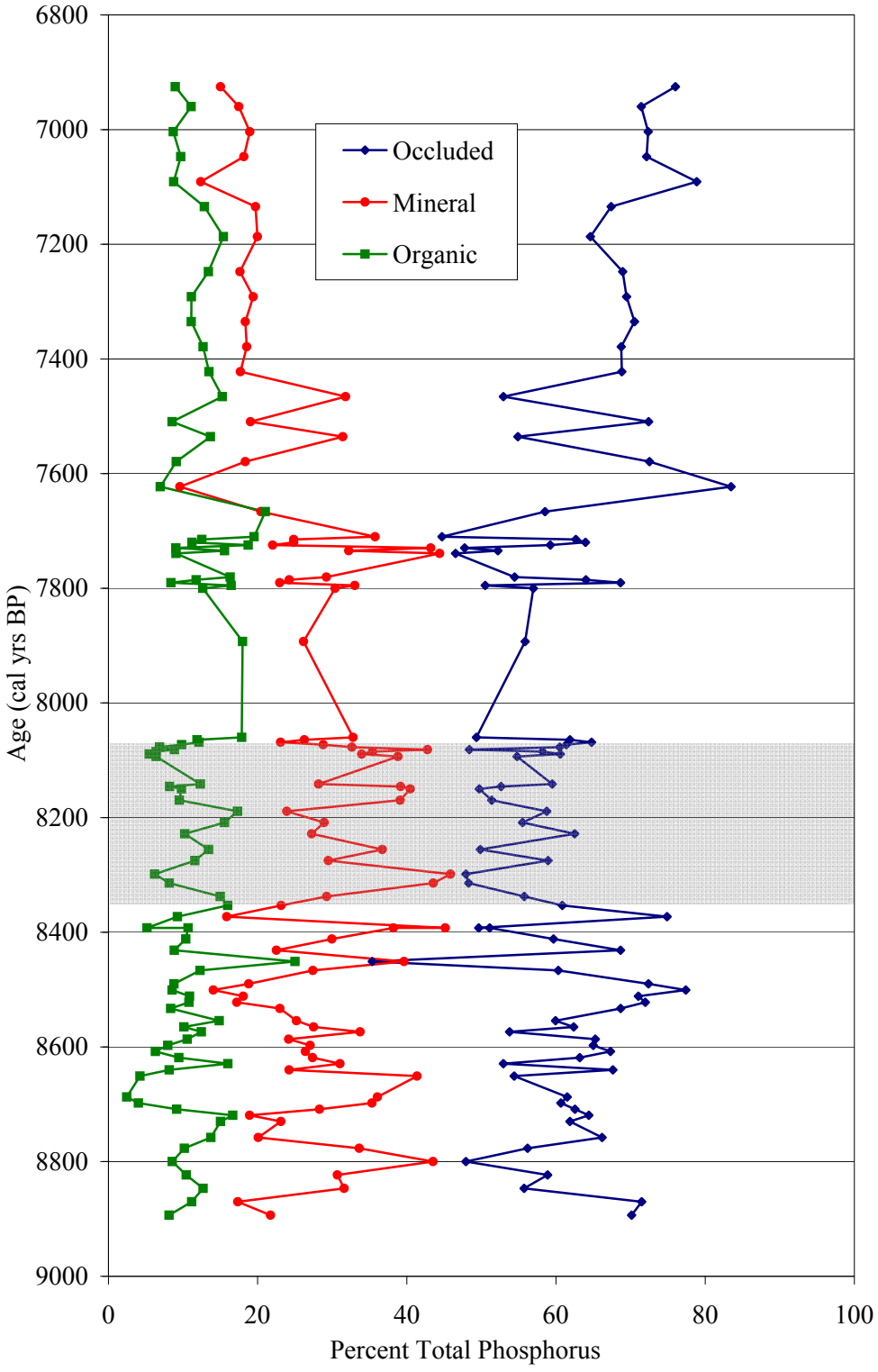

Figure 8. Dry Lake percent total phosphorus. The 8.2 kyr event is shaded in grey.

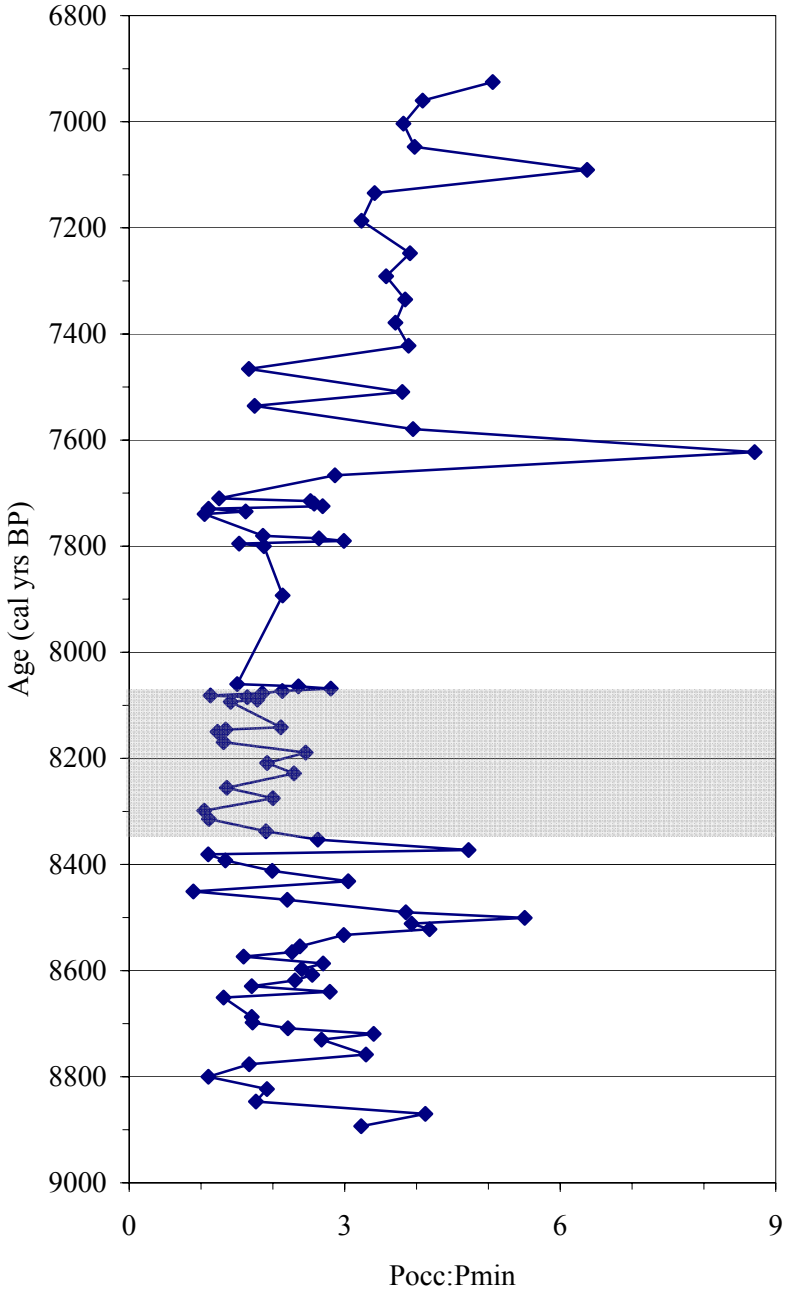

Figure 9. Dry Lake ratio of occluded phosphorus concentration to mineral phosphorus concentration. The 8.2 kyr event is shaded in grey.

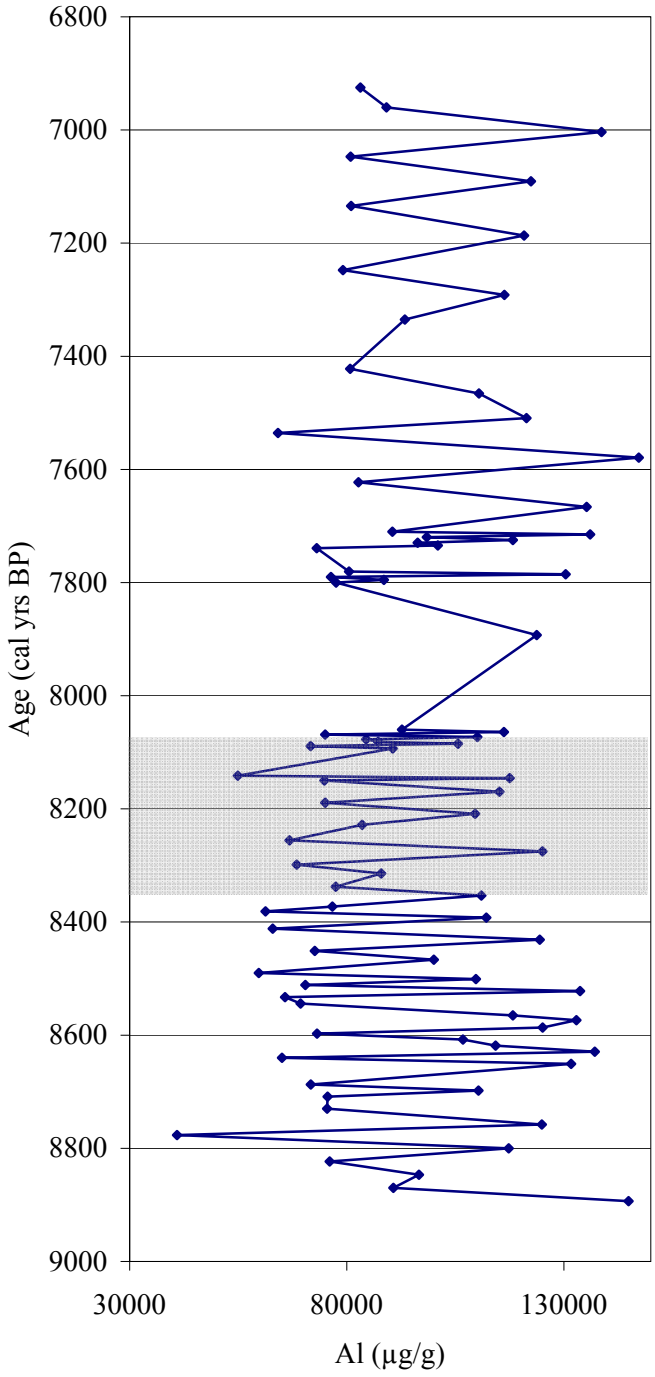

Figure 10. Dry Lake aluminum geochemistry data. The 8.2 kyr event is shaded in grey.

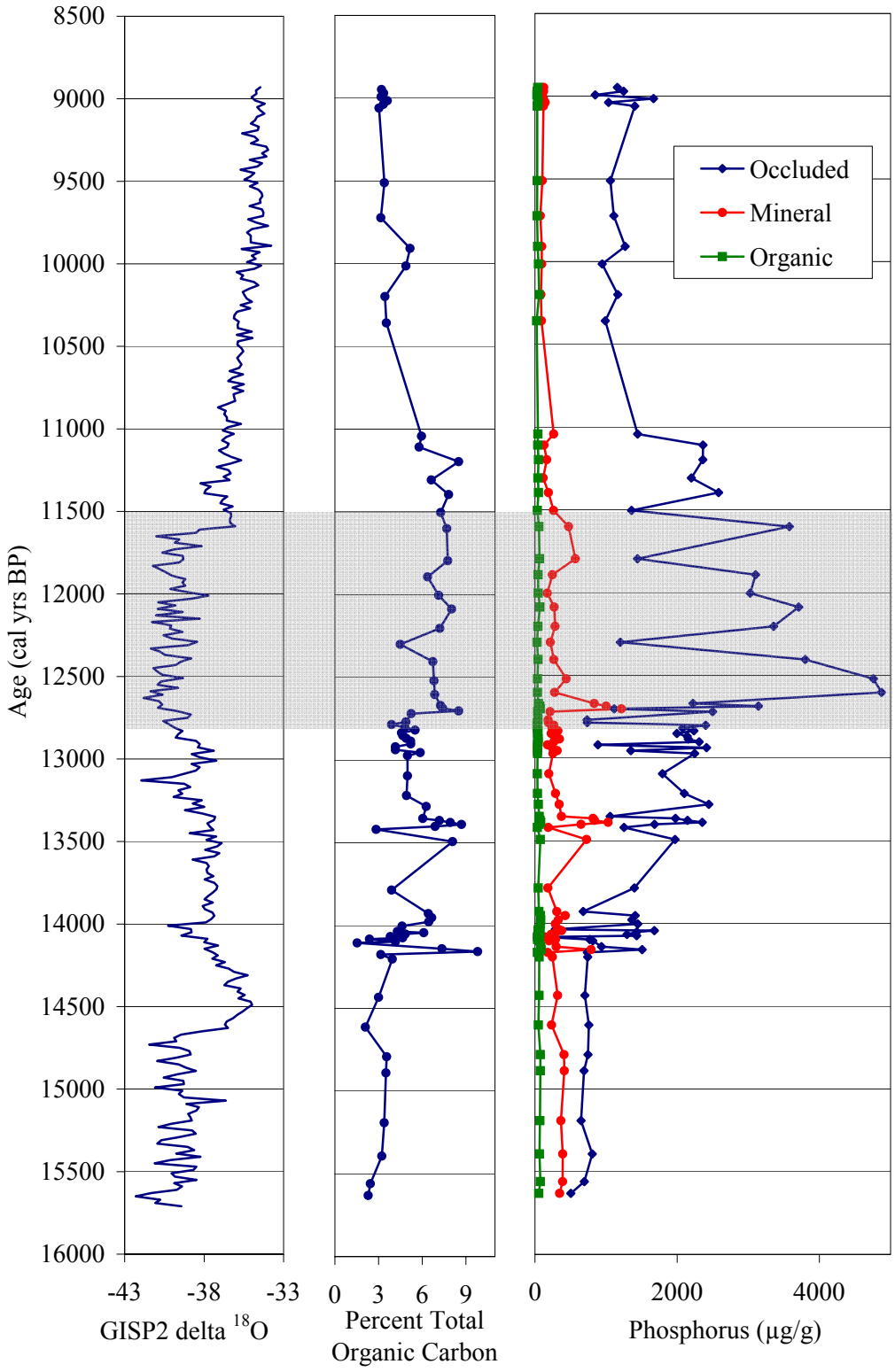

Figure 11. Crystal Lake phosphorus concentration, percent total organic carbon, and GISP2 ice core data. The Younger Dryas is shaded in grey.

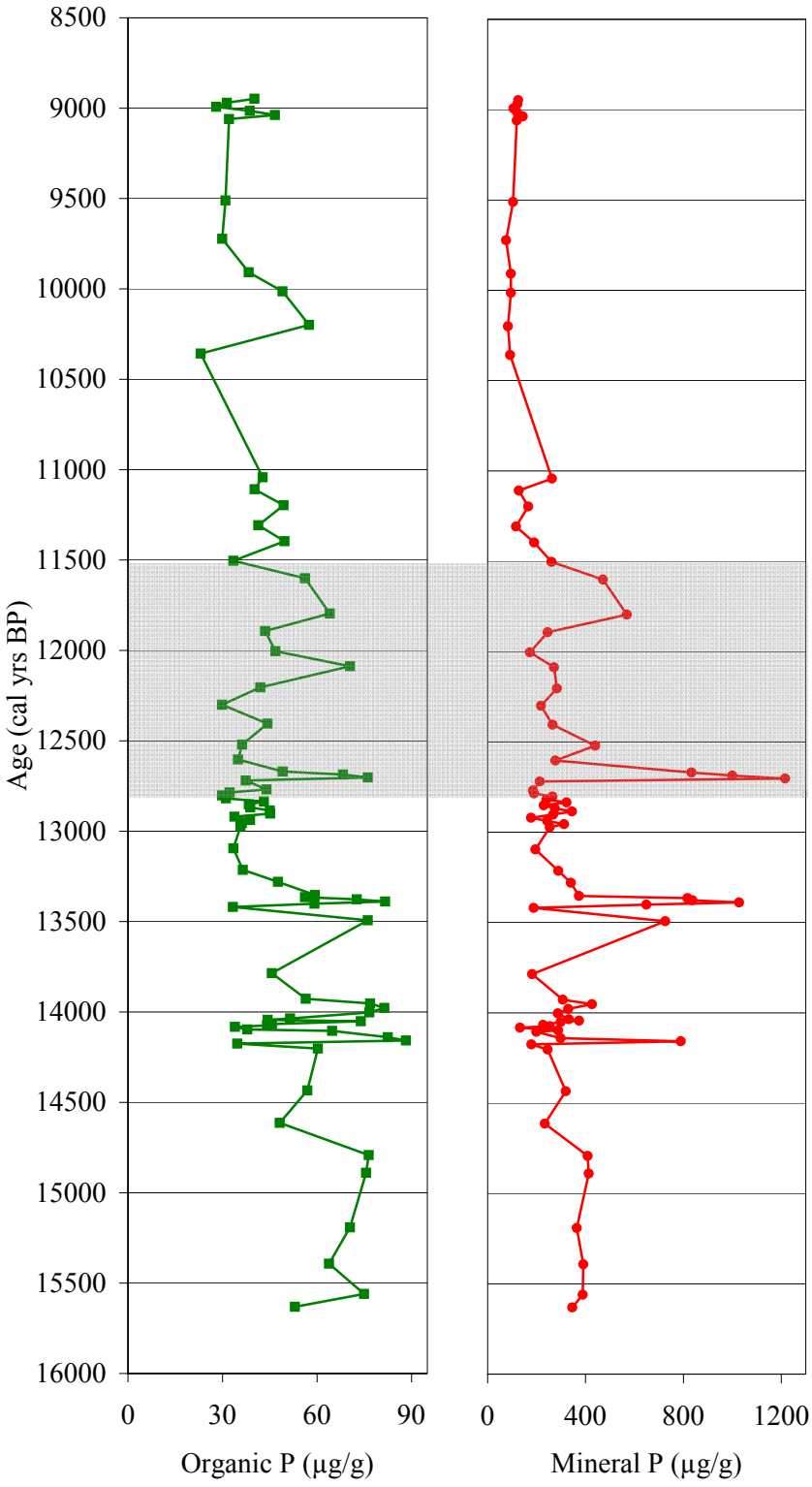

Figure 12. Crystal Lake organic and mineral phosphorus concentration. The Younger Dryas is shaded in grey.

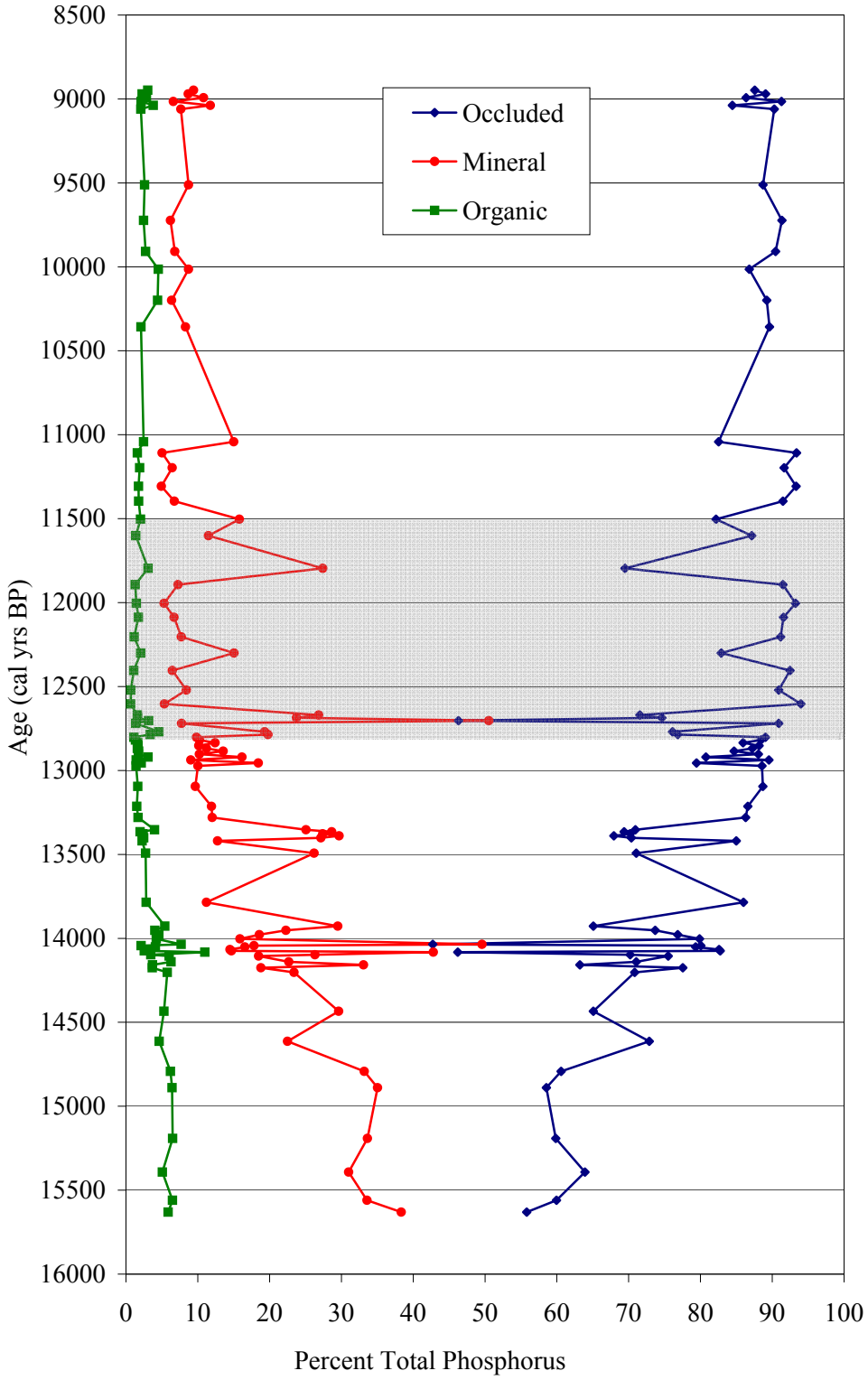

Figure 13. Crystal Lake percent total phosphorus. The Younger Dryas is shaded in grey.

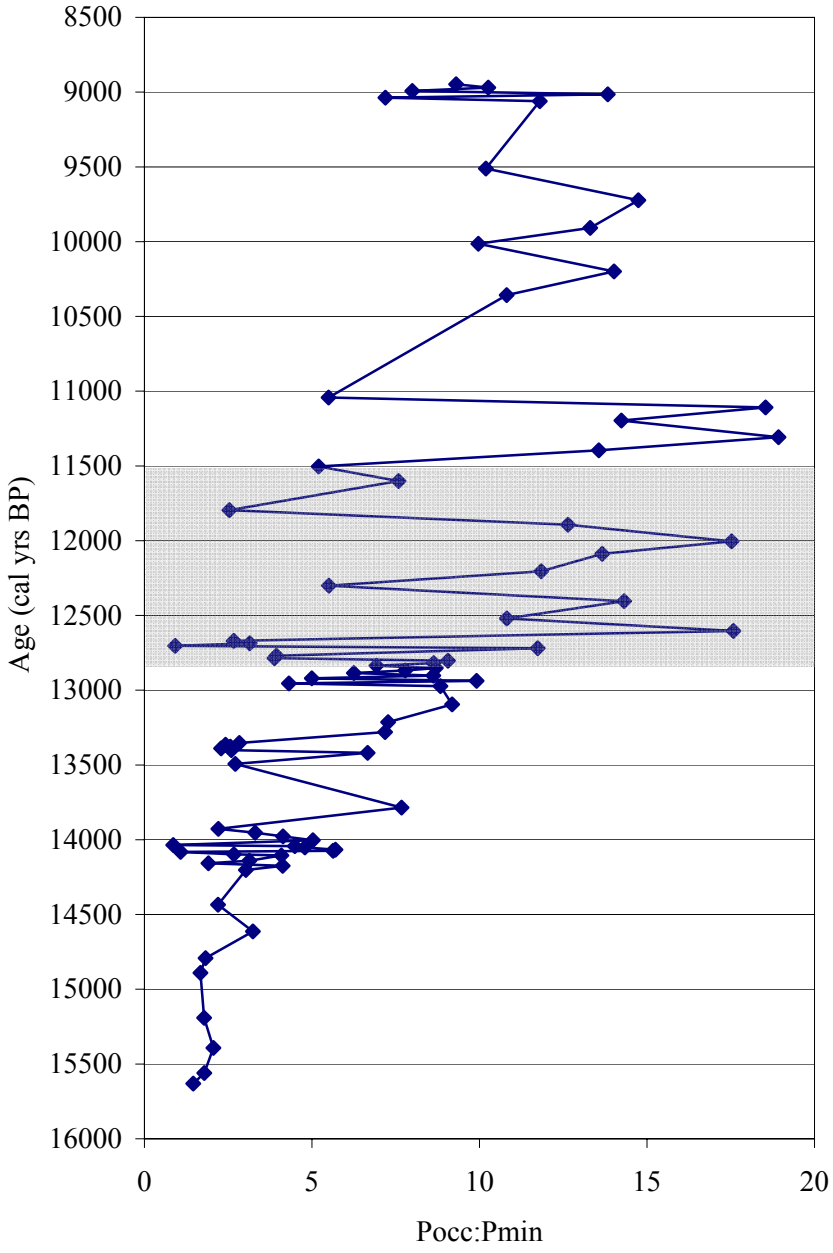

Figure 14. Crystal Lake ratio of occluded phosphorus concentration to mineral phosphorus concentration. The Younger Dryas is shaded in grey.

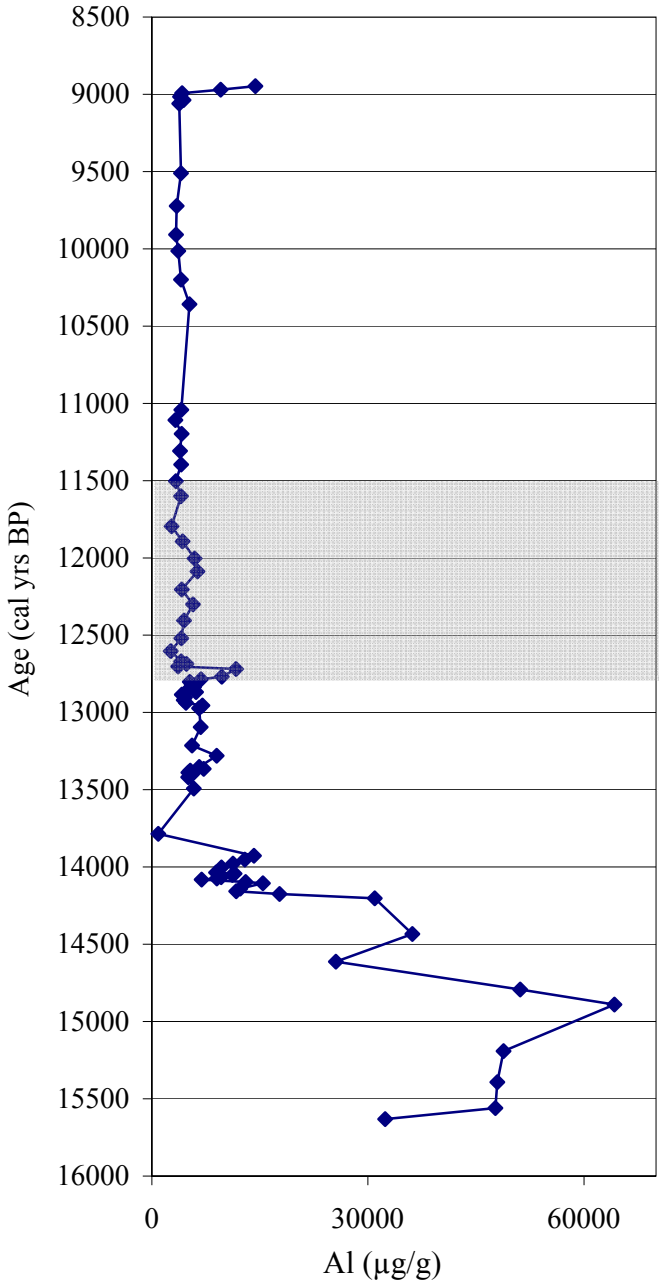

Figure 15. Crystal Lake aluminum concentration. The Younger Dryas is shaded in grey.

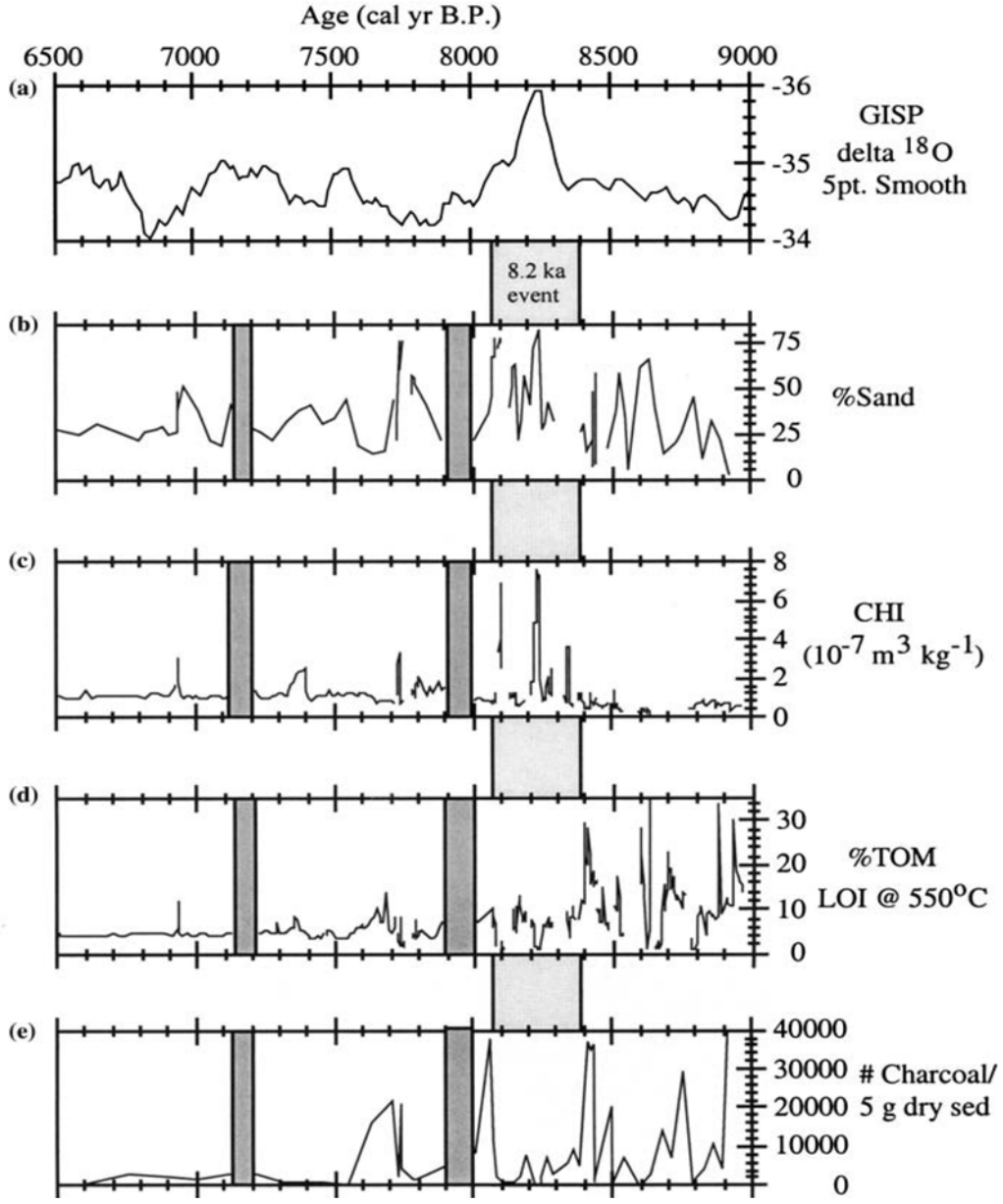

Figure 16. Dry Lake comparison of (a) GISP delta 18O, (b) %Sand, (c) CHI, (d) %TOM, and (e) charcoal grains per 5 g of dry sediment (reprinted from Bird and Kirby, 2006). Light grey box denotes the 8.2 kyr event; dark grey boxes denote gaps attributed to the coring process.

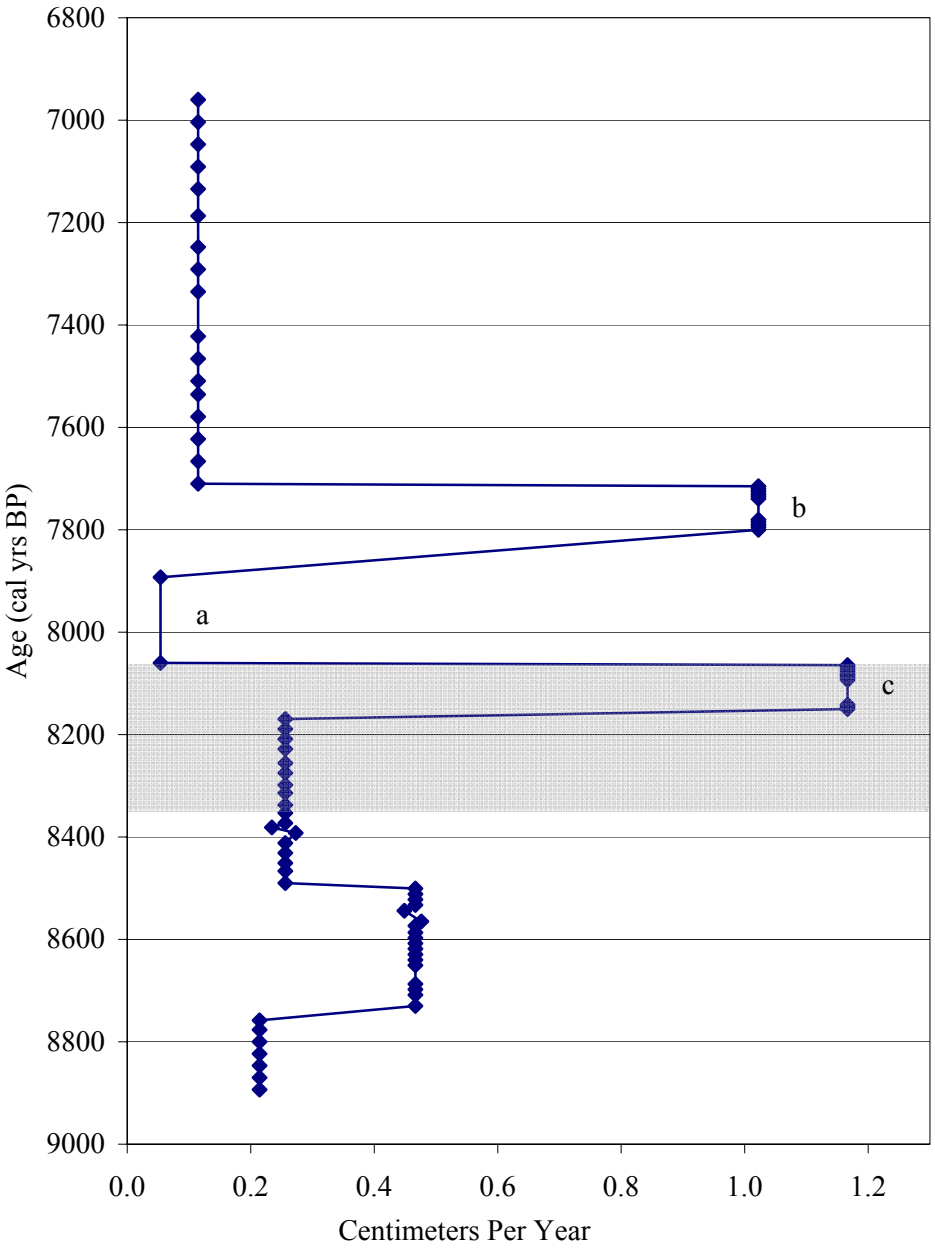

Figure 17. Dry Lake sediment accumulation assuming linear sedimentation rates between carbon dates. Periods labeled a, b, and c are atypical sedimentation rates. The 8.2 kyr event is shaded in grey.

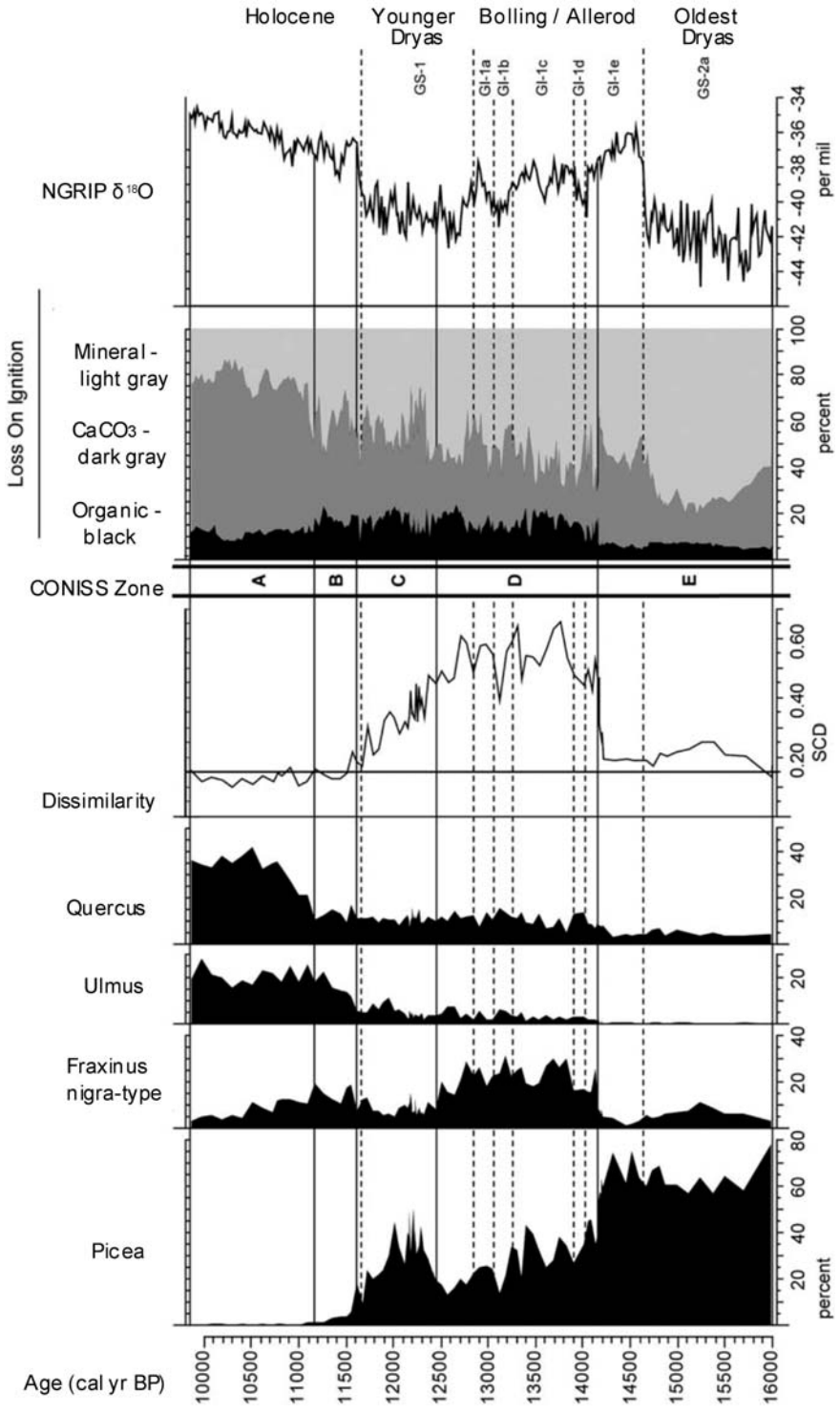

Figure 18. Crystal Lake summary of vegetation during the late Pleistocene (reprinted from Gonzales & Grimm, 2009).

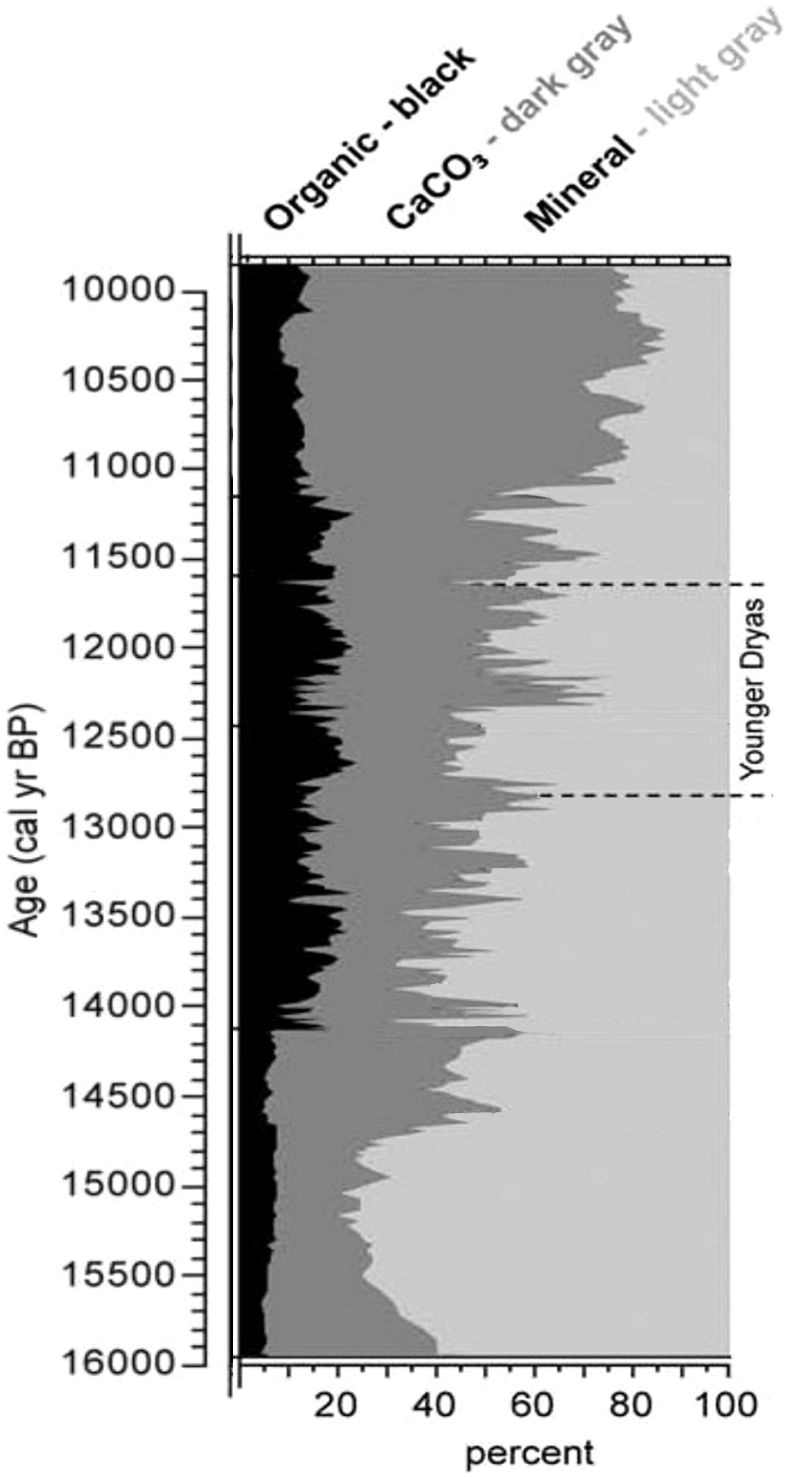

Figure 19. Crystal Lake loss on ignition data (based on Gonzales & Grimm, 2009).

REFERENCES

Alley, R., Marotzke, R., Nordhaus, W., Overpeck, J., Peteet, D., Pielke Jr., R., Pierrehumbert, R., Rhines, P., Stocker, T., Talley, L., Wallace, J. 2003. Abrupt climate change. Science, v. 299, p. 2005-2010.

Alley, R.B., Mayewski P.A., Sowers, T., Stuiver, M., Taylor, K.C., Clark P.U. 1997. Holocene climate instability: a prominent, widespread event 8200 yr ago. Geology, v. 25, p. 483-486.

Alvarez, L.W., Alvarez, W., Asaro, F., Michel, H. 1980. Extraterrestrial cause for the Cretaceous-Tertiary extinction. Science, v. 208, p. 1095-1108.

Bakke, J., Lie, O., Heegaard, E., Dokken, T., Haug, G., Birks, H., Dulski, P., Nilsen, T. 2009. Rapid oceanic and atmospheric changes during the Younger Dryas cold period. Nature Geoscience DOI: 10.1038/NGEO, p. 439.

Bertrand S., Charlet F., Charlier B., Renson V., Fagel N. 2007. Climate variability of southern Chile since the Last Glacial Maximum: a continuous sedimentological record from Lago Puyehue (40°S). Journal of Paleolimnology doi:10.1007/s10933-007-9117y.

Bird, B. and Kirby, M. 2006. An alpine lacustrine record of early Holocene North American monsoon dynamics from Dry Lake, southern California (USA). Journal of Paleolimnology, v. 35, p. 179-192.

Bird, B., Kirby, M., Howat, I., Tulaczyk, S. 2009. Geophysical evidence for Holocene lake-level change in southern California (Dry Lake). Boreas, 10.1111/j.1502-3885.2009.00114.x. ISSN 0300-9483.

Bradbury, J. 1986. Late Pleistocene and Holocene paleolimnology of two mountain lakes in western Tasmania. The Society of Economic Paleontologists and Mineralogists (Research Report), p. 381-388.

Cheng, H., Fleitmann, D., Edwards, R.L., Burns, S.J., Matt, A. 2008. Timing of the 8.2-kyr event in a stalagmite from Northern Oman. PAGES News, v. 16:3, p. 29-30.

Clapperton, C., Hall, M., Mothes, P., Hole, M., Still, J., Helmens, K., Kuhry, P., Gemmell, A. 1997. A Younger Dryas Icecap in the Equatorial Andes. Quaternary Research, v. 47, p. 13-28.

Curry, B.B. 2005. Surficial Geology of Crystal Lake Quadrangle, McHenry and Kane Counties, Illinois: Illinois State Geological Survey, Illinois Geologic Quadrangle Map, IGQ Crystal Lake-SG, 1:24,000.

Curry, B.B. 2005. Drift Thickness Map of Crystal Lake Quadrangle, McHenry and Kane Douglas Counties, Illinois: Illinois State Geological Survey, Illinois Geologic Quadrangle Map, IGQ Crystal Lake-DT, 1:24,000.

Curry, B.B. 2005. Data Point Locations of Crystal Lake Quadrangle, McHenry and Kane Counties, Illinois: Illinois: Illinois State Geological Survey, Illinois Geologic Quadrangle Map, IGQ Crystal Lake-DP, 1:24,000.

Curry, B.B. 2005. Bedrock Topography of Crystal Lake Quadrangle, McHenry and Kane Counties, Illinois: Illinois: Illinois State Geological Survey, Illinois Geologic Quadrangle Map, IGQ Crystal Lake-BT, 1:24,000.

Dowdeswell, J.A. and White, J.W.C. 1995. Greenland ice core records and rapid climate change. Philosophical Transactions of The Royal Society, Series A, v. 352, p. 359-371.

Fairbanks, R.G. 1989. A 17,000-year glacio-eustatic sea level record: influence of glacial melting rates on the Younger Dryas event and deep-ocean circulation. Nature, v. 342, p. 637-642.

Filippelli, G. and Souch, C. 1999. Effects of climate and landscape development on the terrestrial phosphorus cycle. Geology, v. 27, p. 171-174.

Filippelli, G., Souch, C., Menounos, B., Slater-Atwater, S., Jull, A.J.T., Slaymaker, O. 2006. Alpine lake sediment records of the impact of glaciation and climate change on the biogeochemical cycling of soil nutrients. Quaternary Research, v. 66, p. 158-166.

Firestone, R., West, A., Kennett, J., Becker, L., Bunch, T., Revay, Z., Schultz, P., Belgya, T., Kennett, D., Erlandson, J., Dickenson, O., Goodyear, A., Harris, R., Howard, G., Kloosterman, J., Lechler, P., Mayewski, P., Montgomery, J., Poreda, R., Darrah, T., Hee, S., Smith, A., Stich, A., Topping, W., Wittke, J., Wolbach, W. 2007. Evidence for an extraterrestrial impact 12,900 years ago that contributed to the megafaunal extinctions and the Younger Dryas cooling. Proceedings of the National Academy of Sciences, v. 104, p. 16016-16021.

Gonzales, L. and Grimm, E. 2009. Synchronization of late-glacial vegetation changes at Crystal Lake, Illinois, USA with the North Atlantic Event Stratigraphy. Quaternary Research doi:10.1016/j.yqres.2009.05.001.

Hillaire-Marcel, C., de Vernal, A., Piper, D.J.W. 2007. Lake Agassiz Final drainage event in the northwest North Atlantic. Geophysical Research Letters, v. 34, L15601, doi:10.29/2007GLE030396.

Ljung, K., Bjorck, S., Renssen, H., Hammarlund, D. 2008. South Atlantic island record reveals a South Atlantic response to the 8.2 kyr event. Climate of the Past, v. 4, p. 35-45.

Marotzke, J. 2000. Abrupt climate change and thermohaline circulation: Mechanisms and predictability. Proceedings of the National Academy of Sciences, v. 97:4, p. 1347-1350.

Meese, D., Alley, R., Fiacco, R., Germani, M., Gow, A., Grootes, P., Illing, M., Mayewski, P., Morrison, M., Ram, M., Taylor, K., Yang, Q., Zielinski, G. 1994. Preliminary depth-age scale of the GISP2 ice core. Special Cold Regions Research and Engineering Laboratory Report 94-01.

Midwestern Regional Climate Center. 2000. Precipitation/Temperature Summary Station 115326 Marengo, IL. http://mrcc.isws.illinois.edu/. Accessed June 15, 2010.

Rohling, E. and Palike, H. 2005. Centennial-scale climate cooling with a sudden cold event around 8,200 years ago. Nature, v. 434, p. 975-979.

Sasman, R.T. 1957. The water level problem at Crystal Lake, McHenry County. Illinois State Water Survey, Champaign, IL, ISWS RI-32.

Schlesinger, W.H. 1997. Biogeochemistry: An Analysis of Global Change, 2nd ed. Academic Press, San Diego, p. 98.

Stuiver, M., Grootes, P.M., Braziunas, T.F. 1995. The GISP2 d18O climate record of the past 16,500 years and the role of the sun, ocean and volcanoes. Quaternary Research, v. 44, p. 341-354.

Tiessen, H. and Moir, J.O. 1993. Characterization of Available P by Sequential Extraction. In: Soil Sampling and Methods of Analysis (ed. M.R. Carter), Lewis Publishers, Boca Raton, FL, p. 75-86.

Vitousek, P.M. and Farrington, H. 1997. Nutrient limitation and soil development: experimental test of a biogeochemical theory. Biogeochemistry, v. 37, p. 63-75.

Walker, T.W. and Syers, J.K. 1976. The fate of phosphorus during pedogenesis. Geoderma, v. 15, p. 1-19.

Western Regional Climate Center. 2009. Big Bear Lake, California 040741. Period of Record Monthly Climate Summary. http://www.wrcc.dri.edu/. Accessed Jun 15, 2010.

CURRICULUM VITAE

James Brice Mabry

EDUCATION:

M.S. Geology, December 2011
Indiana University Purdue University - Indianapolis, IN
Thesis: The impact of glaciation and climate change on biogeochemical cycling and landscape development

B.A. Economics, May 1999
Indiana University Purdue University - Indianapolis, IN

WORK AND FIELD EXPERIENCE:

Geology Department Biogeochemical Lab Assistant - IUPUI 2008-2010
Duties include lab equipment maintenance, Leeman Labs ICP operation, full acid digestion, phosphorus extraction, Shimadzu spectrophotometer operation, mercury determination

RX Exploration, Inc. - Marysville, MT May-June 2009
Participated in mine mapping and core logging for gold exploration

Gentor Resources, Inc. - Patterson, ID July-August 2008
Collected soil samples for molybdenum exploration

IUPUI Field Work - Victorville, CA April 2006
Mineral collection, identification, and thin section preparation of ignimbrite samples

LABORATORY EQUIPMENT:

Leeman Labs ICP Spectrometer
Shimadzu UV-2401PC Spectrophotometer
Transmitting and reflected light polarizing microscopes
Malvern Laser Particle Size Analyzer
Leco AMA254 Mercury Analyzer

CONFERENCES ATTENDED:

2008 Geological Society of America Annual Meeting, Houston, TX
2007 Geological Society of America Annual Meeting, Denver, CO